JACS
JOURNAL OF THE AMERICAN CHEMICAL SOCIETY

Communication

pubs.acs.org/JACS

Mild-Temperature $Mn_2(CO)_{10}$-Photomediated Controlled Radical Polymerization of Vinylidene Fluoride and Synthesis of Well-Defined Poly(vinylidene fluoride) Block Copolymers

Alexandru D. Asandei,* Olumide I. Adebolu, and Christopher P. Simpson

Institute of Materials Science and Department of Chemistry, University of Connecticut, Storrs, Connecticut 06069-3136, United States

Supporting Information

ABSTRACT: By contrast to typical high-temperature (100−250 °C) telo-/polymerizations of gaseous fluorinated monomers, carried out in high-pressure metal reactors, the visible light, $Mn_2(CO)_{10}$-photomediated initiation of vinylidene fluoride (bp = −83 °C) polymerization occurs readily from a variety of alkyl, semifluorinated, and perfluorinated halides at 40 °C, in low-pressure glass tubes and in a variety of solvents, including water and alkyl carbonates. Perfluorinated alkyl iodide initiators also induce a controlled radical polymerization via iodine degenerative transfer (IDT). While IDT proceeds with accumulation of the less reactive P_m-CF_2-CH_2-I vs the P_n-CH_2-CF_2-I chain ends, $Mn_2(CO)_{10}$ enables their subsequent quantitative activation toward the synthesis of well-defined poly(vinylidene fluoride) block copolymers with a variety of other monomers.

Fluorinated (co)polymers are fundamental specialty materials with a wide range of high-end applications[1] requiring their precise synthesis. However, while novel controlled radical polymerization (CRP) methods[2] (atom transfer, nitroxide, or addition−fragmentation) have recently seen remarkable developments[2,3] and have proven very effective for (meth)acrylates or styrene, their applicability in the CRP of main-chain fluorinated alkene monomers (FMs: vinylidene fluoride (VDF), hexafluoropropene (HFP), tetrafluoroethylene, etc.) still awaits demonstration.

The most successful approach to FM-CRP[1] has emerged from high-temperature (100−250 °C) free radical VDF telomerizations[4] with polyhalides,[1a−c] especially (per)-fluorinated iodine chain-transfer (CT) agents,[5−9] and is mechanistically based on one of the oldest CRP methods,[10] the iodine degenerative transfer[3,11] (IDT: $P_n^\bullet + P_m$-I ⇌ P_n-I + $P_m^\bullet$).[1,5]

However, IDT always requires a free radical source (e.g., *tert*-butyl peroxide),[1,4,5,7] as *direct* metal-catalyzed initiation from perfluoroalkyl iodides (R_F-I) or any other halides is not available. Indeed, while such electrophilic $R_F^\bullet$ radicals add readily to alkenes using Cu, Pd, or Ti catalysts,[12] their addition to electrophilic, fluorinated substrates (FMs) at T < 100 °C, and especially at room temperature (rt), is lacking. Conversely, while VDF polymerization can be initiated at rt,[13] only very low VDF oligomers (DP = 1−3) may be obtained, even at T > 100 °C from transition metal salts and polyhalides,[1,5,14] and there are no reports on metal-mediated FM/VDF polymerizations, let alone VDF-CRP. Moreover, by contrast to the CRP of acrylates or styrene, VDF-IDT produces *two* halide chain ends, P_n-CH_2-CF_2-I and P_m-CF_2-CH_2-I, with widely different reactivity.[8]

Thus, the ability to initiate *directly* from halides, mediate rt FM-CRP, and activate *both* PVDF-I termini would be of great value in the controlled synthesis of well-defined block, graft, and star FM structures, which, due to the current lack of such chemistry, inevitably end up as mixtures of homo- and copolymers.

Consequently, the study of FM-CRPs and the synthesis of complex architectures thereby derived is a worthy[1,5−8] yet very challenging endeavor, especially on a laboratory scale, as VDF boils at −83 °C, and typical telo-/polymerizations are carried out at 100−250 °C.[1] Accordingly, while styrene or acrylate CRPs can easily be sampled on a 1 g scale, kinetics of VDF polymerizations involve many time-consuming one-data-point experiments in expensive high-pressure metal reactors, which require at least tens of grams of monomer. Thus, development of methods allowing polymerizations to proceed at mild temperatures in inexpensive pressure glass tubes would be highly desirable, as such methods could be easily adapted for fast catalyst and reaction condition screening and take advantage of photochemistry.

As such, while VDF telomerizations under high-power UV are available,[1,5,15] there are no reports on VDF polymerizations under regular *visible* light. To this end, we decided to investigate mild photochemical means of radical generation,[16] such as transition-metal-mediated photopolymerizations using low wattage (<30 W), spiral, compact white light fluorescent bulbs.

Since VDF is a very reactive monomer, effective rt initiators should provide highly reactive radicals. Conversely, the visible-light-generated metalloradical should be a very good halide abstractor. Prototypical examples[16] are $(CO)_n$Mt-Mt$(CO)_n$-type dimers, where the inexpensive $Mn_2(CO)_{10}$[17a] is the most popular.[16] The Mn−Mn linkage is weak (20−40 kcal/mol),[16,17b] and rt visible light photolysis provides the $Mn(CO)_5^\bullet$ 17e$^-$ metalloradical with good quantum efficiency.[18]

$Mn(CO)_5^\bullet$ cleanly abstracts halides from a variety of substrates,[16c] reacting faster with primary rather than secondary

Received: January 6, 2012
Published: March 29, 2012

   dx.doi.org/10.1021/ja300178r | *J. Am. Chem. Soc.* 2012, 134, 6080−6083

or tertiary ones, yet there are no examples with semi- or perfluoroalkyl substrates. Moreover, while $Mn_2(CO)_{10}/CCl_4$-initiated polymerizations were developed in the 1960s,[19] $Mn_2(CO)_{10}$ was only recently employed in other free radical polymerizations (FRP),[20] and especially in the photomediated IDT of vinyl acetate (VAc) and its copolymers,[21] where $Mn(CO)_5^\bullet$ activates an alkyl iodide initiator, but the resulting $Mn(CO)_5$-I is not involved in the reversible I transfer. We thus decided to assess its scope and limitations for FM-CRPs and optimize the system.

While visible light could also be invoked in the photodissociation of RX, control experiments (Table S1, exp. 1−4) revealed no polymerization in the dark, or with illumination in the absence of $Mn_2(CO)_{10}$. Though polymerizations could easily be carried out anywhere from T = 0 to 100 °C, (Table S1, exp. 6−12), we selected T = 40 °C for all further experiments as a good compromise between rate, minimization of possible higher temperature side reactions, and a safe pressure inside the tube. In fact, simply lowering the bottom part of the light bulb inside the oil bath (Figure S1) helped maintain such temperature, with minimal additional heating from the hotplate.

Typical VDF reactions are carried out in the non-solvent acetonitrile (ACN),[1,4−8] but there is very little data[22] on the solvent effect in VDF polymerizations, let alone photopolymerizations. Thus, we first surveyed a large number of solvents (Table S2), noting that minimization of solvent CT outweighs solubility considerations. Indeed, all good PVDF solvents[23a] (DMF, DMAC, etc.) acted as strong CT agents and led to very low conversions. By contrast, while fast polymerizations could be carried out even in water, remarkable trends were observed with carbonates, especially dimethyl carbonate (DMC), a green solvent.[23b] Indeed, although DMC does not dissolve PVDF at rt, and similarly to that with ACN, the reaction displays typical features of heterogeneous polymerizations of gaseous monomers,[23c] it provides by far the fastest reaction rates, at least 5 times those obtained in ACN. As DMC is stable to photolysis,[24] this is not a photosensitizing effect, but a consequence of low CT, better monomer solubilization, and polymer swelling,[25] which enables faster monomer diffusion to the propagating center.

The proposed reaction mechanism is outlined in Scheme 1, and the polymerization setup is illustrated in Figure S1. Following photolysis of $Mn_2(CO)_{10}$ (eq 1), irreversible[21] halide abstraction from R-X (driven by the formation of high bond dissociation energy (BDE) Mn-X, X = Cl, Br, I, eq 2)[26] affords $Mn(CO)_5$-X and $R^\bullet$, which, if reactive enough, initiates VDF polymerization (eq 3). As VDF is asymmetrical, both 1,2- and 2,1-modes of propagation (eq 4, head-to-tail, HT, ∼95%,[1,6,22] and respectively head-to-head, HH) are possible in FRPs.

Out of all halides investigated (Chart S1, Table S1), most of which were *never previously reported in conjunction with* $Mn_2(CO)_{10}$, reactive alkyl polyhalides, as well as semi- and perfluorinated halides such as $CHCl_3$, CCl_4, CCl_3-Br, CCl_3-CCl_3, $CF_3(CF_2)_2CO$-Cl, CF_3-SO_2-Cl, Cl-CF_2-CClF-Cl, Cl-$(CF_2)_8$-Cl, -$(CF_2$-$CFCl)_n$-, EtOOC-CF_2-Br, Br-CF_2-CH_2-CF_2-Br, Br-$(CF_2)_4$-Br, CH_3-I, $CH_3(CH_2)_5$-I, I-$(CH_2)_{10}$-I, C_6F_5-CF_2-I, H-CF_2-CF_2-CH_2-I, EtOOC-CF_2-I, Cl-CF_2-CFCl-I, CF_3-I, CF_3CF_2-I, $(CF_3)_2CF$-I, $(CF_3)_3C$-I, $CF_3(CF_2)_3$-I, and I-$(CF_2)_{4,6}$-I, all led to polymer formation, as demonstrated (NMR) in Figure S2 and Table S3. Remarkably, initiation is afforded not only from polyhalides and all R_F-I structures (which also provide VDF-IDT *vide infra* and dramatic reduction of HH defects, Figure S2b) but also from semifluorinated chain end models, and especially from simple inactivated alkyl iodides, thus indicating the feasibility of initiating block or graft VDF copolymerization *directly* from the corresponding initiators anchored on polymeric chains, surfaces, etc. Initiation is demonstrated not only for VDF but also for CF_2=CFCl, CF_2=CCl_2, CF_2=CFBr, CH_2=CFH, and VDF random copolymers with CF_2=$CF(CF_3)$ and CF_2=$CF(OCF_3)$ (Table S1).

Subsequently, the polymerization outcome is controlled by the carbon−halide bond strength, which determines the RX CT ability (eqs 5 and 6). Accordingly, the initiators fall into three classes which require different amounts of $Mn_2(CO)_{10}$ for activation, and VDF undergoes conventional FRP for RX (X = Cl, Br, I) and IDT-mediated CRP for R_F-I.

Thus, initiators with strong R-X bonds (alkyl iodides, $CHCl_3$, R_F-Cl) do not undergo noticeable CT with $PVDF^\bullet$, demand stoichiometric $Mn_2(CO)_{10}$ activation, and afford PVDF with no halide chain ends (Figure S2). By contrast, substrates with weak R-X bonds (e.g., CF_3SO_2-Cl, C_2Cl_6, CCl_4, CCl_3Br, R_F-X, X = Br, I) *do undergo* CT to the initiator (eqs 5 and 6), require reduced (10%) amounts of $Mn_2(CO)_{10}$, and afford halide-functionalized PVDF-X (X = Cl, Br, I, Figure S2). However, while good Cl and Br CT agents can at best provide efficient telomerizations,[4] uncatalyzed halide DT-CRP occurs only for iodine. As such, high-CT R_F-I initiators suitable for IDT-CRPs[5] are converted early in the process into macromolecular PVDF-I CT agents,[8] where the terminal P_m-CF_2-CH_2-I[5−9] 2,1-unit is about 25 times less reactive toward IDT than the isomeric P_n-CH_2-CF_2-I 1,2-unit.[8]

Once all the R_F-I initiator is consumed via CT, no new PVDF-I chains are generated, and the thermodynamically neutral, *reversible* I exchange (IDT, K_{equil} = 1) between equally reactive, propagating and dormant P_n-CH_2-$CF_2^\bullet$ and P_m-CH_2-CF_2-I terminal 1,2-units (eq 7) is in operation. This enables IDT-CRP, as demonstrated (Figures 1 and S3, VDF; Figure S4, VDF-*co*-HFP) by the linear dependence of M_n on conversion and moderate polydispersity index (PDI) values, which indicate that $Mn_2(CO)_{10}$ supports a photo-CRP over a wide range of molecular weights (M_n = 1000−25 000). However, such CRP toward higher M_n values is kinetically impractical under these conditions.

While IDT catalysis would lead to a PDI decrease,[3,11] control experiments (Figure S5) reveal that, consistent with PVAc-

Scheme 1. $Mn_2(CO)_{10}$-Photomediated VDF-CRP

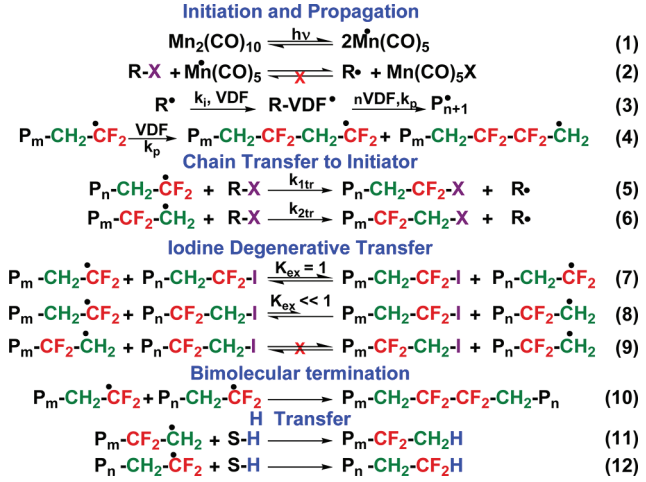

dx.doi.org/10.1021/ja300178r | J. Am. Chem. Soc. 2012, 134, 6080−6083

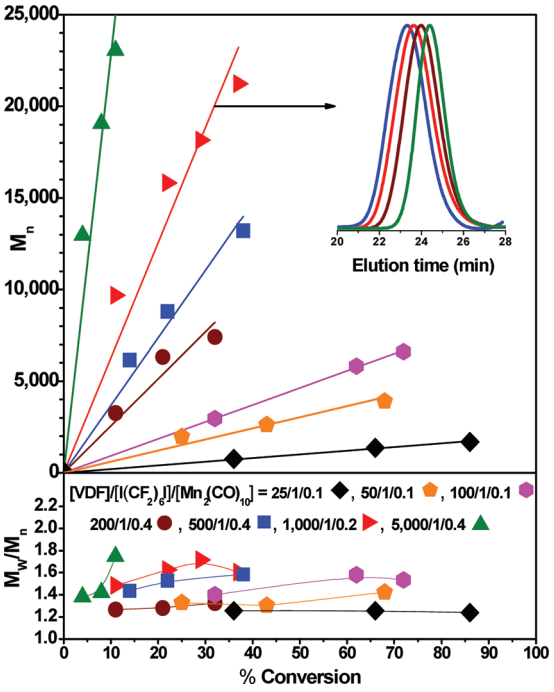

Figure 1. Dependence of M_n and M_w/M_n on conversion in $Mn_2(CO)_{10}$-photomediated VDF-IDT. Inset: GPC traces for $[VDF]/[I(CF_2)_6I]/[Mn_2(CO)_{10}]$ = 1000/1/0.2 trace.

IDT,[21] the photochemically inactive[27a] $Mn(CO)_5$-I is incapable of reversibly transferring I. Conversely, although R_F-$Mn(CO)_5$ (R_F = CH_2F, CF_2H)[27b] are known, organometallic CRP mediation by PVDF-$Mn(CO)_5$ can be discounted on the basis of the observed -I, not -H or -$Mn(CO)_5$ chain ends, of the successful CRP with *catalytic*, not stoichiometric $Mn_2(CO)_{10}$ vs R_F-I, and considering the BDE order (R_F-$Mn(CO)_5$ < $(CO)_5$Mn-$Mn(CO)_5$ < R_F-I < I-$Mn(CO)_5$, i.e., 34,[27b] 38,[26b] 48,[28] and 54 kcal/mol[26]), consistent with the instability of Mn alkyls under irradiation.[26b]

In IDT, HH defects are dramatically suppressed (Figure S2), being intercepted as P_m-CF_2-CH_2-I. I-R_F-I initiators are particularly suitable for FM-CRPs, as bidirectional growth from difunctional propagating species,[10] in conjunction with initiator or chain-end halide activation by the continuously photogenerated $Mn(CO)_5^{\bullet}$ [18b] (eq 2), compensates for termination by radical coupling[10] and maintains a steady-state radical concentration.

However, due to the much stronger -CH_2-I bond, the cross-IDT between the 1,2- and 2,1- units (eq 8) is shifted toward the irreversible buildup of P_n-CF_2-CH_2-I chain ends, whereas the IDT of the 2,1-terminal units is virtually non-existent (eq 9).[7,8]

Although these are unavoidable features in conventional IDT as well,[7,8] while the concentration of active -CH_2-CF_2-I termini decreases and unreactive -CF_2-CH_2-I species accumulate with conversion (Figure S6) and contribute to PDI broadening,[8,9,21] the *total* (-CH_2-CF_2-I + -CF_2-CH_2-I) iodine functionality remains at least 95%, even at larger levels of $Mn_2(CO)_{10}$, which is quite adequate for block copolymer synthesis, on the condition that *both* halide chain ends can be activated.

Yet, while high-temperature ethylenation,[29] azidation,[29c] and block copolymer synthesis via ATRP[29d] or IDT[9] were previously attempted from PVDF-I, all such endeavors were fundamentally incomplete, due to the failure of the respective chemistries to activate the stronger and dominant -CF_2-CH_2-I termini. Thus, the products were always inseparable, ill-defined mixtures.

By contrast, $Mn(CO)_5^{\bullet}$ affords the clean and quantitative activation of *both* -CH_2-CF_2-I and -CF_2-CH_2-I chain ends and enables the synthesis of well-defined block copolymers. Selected examples of the associated ^{1}H NMR characterization are presented in Figure 2 and Table S4. In addition to acetone

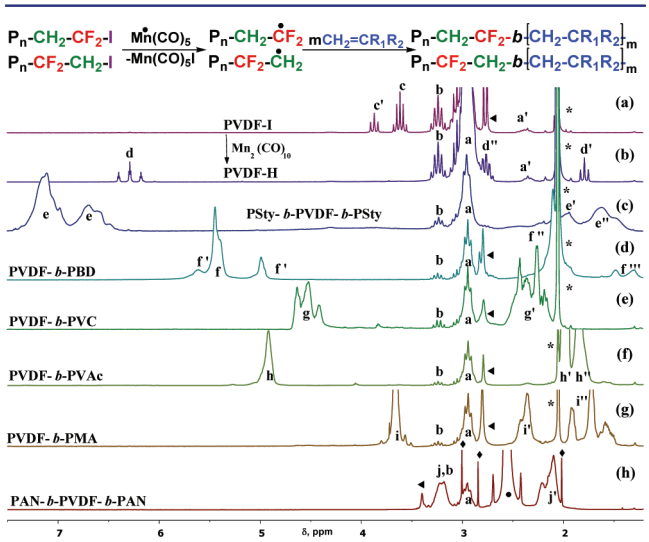

Figure 2. 500 MHz ^{1}H NMR spectra of PVDF-I, PVDF-H, and various PVDF block copolymers. All in d_6-acetone, except PAN in d_6-DMSO. ◀ = H_2O, * = acetone, ♦ = DMAC, ● = DMSO.

and water (δ = 2.05 and 2.84 ppm),[30] the HT -CF_2-[CH_2-CF_2]$_n$-CH_2- (**a**) and HH -CF_2-CH_2-CH_2-CF_2- (**a′**) PVDF linkages[29,31] are observed at δ = 2.8−3.1 and 2.3−2.4 ppm, respectively. Resonance **b** (δ = 3.25 ppm) confirms the R_F-CH_2-CF_2- connectivity with the first polymer unit, and the 1,2-CH_2-CF_2-I (**c**) and 2,1-CF_2-CH_2-I (**c′**) iodine chain ends are seen[7] at δ = 3.62 and 3.87 ppm (Figure 2a).

While VDF-FRP terminates primarily by recombination of 1,2-units (eq 10),[1,4−9] in VDF-IDT, trace termination by H transfer to the propagating chains (eqs 11 and 12, i.e., -CH_2-CF_2-*H* and -CF_2-CH_3, peaks **d**, **d′**) is seen at δ = 6.30 and 1.80 ppm.[31c] Upon treatment of PVDF-I with stoichiometric $Mn(CO)_5^{\bullet}$, complete activation of *both* halide chain ends occurs. Thus, in the absence of a monomer as addition substrate, the resulting radicals are deactivated by H abstraction from solvent to generate the same **d** and **d′** peaks and a more resolved -CH_2-CF_2-CH_2-CF_2-H **d″**, δ = 2.77 ppm[31e] (Figures 2b and S2d,e, ^{19}F NMR).

As such, carrying out the reaction in the presence of a radically polymerizable alkene leads to the first examples of well-defined, AB- or ABA-type PVDF block copolymers with styrene (**e**, **e′**), butadiene (**f**, **f′**, **f″**, **f‴**), vinyl chloride (**g**, **g′**), vinyl acetate (**h**, **h′**, **h″**), methyl acrylate (**i**, **i′**, **i″**), and acrylonitrile (**j**, **j′**), initiated from *both* PVDF halide chain ends (Table S4 and Figure 2c−h). While here $Mn_2(CO)_{10}$ operates simply as a photoactivator and there is no IDT, control of the block copolymerization by other CRP methods can be envisioned.

To summarize, we have demonstrated for the first time, using VDF as a model for main-chain fluorinated gaseous monomers, that the initiation of the polymerization can easily be accomplished at mild temperatures, *directly* from a variety of alkyl, semifluoralkyl, and perfluoroalkyl halides (Cl, Br, I) using

dx.doi.org/10.1021/ja300178r | J. Am. Chem. Soc. 2012, 134, 6080−6083

a visible light, $Mn_2(CO)_{10}$-photomediated protocol, carried out in low-pressure glass tubes, and which is especially successful in DMC. Moreover, in the presence of perfluorinated alkyl iodides, such reactions follow an IDT mechanism, leading to a CRP process. Finally, the $Mn_2(CO)_{10}$-induced complete activation of *both* -CH_2-CF_2-I and -CF_2-CH_2-I halide chain ends affords the first examples of well-defined block copolymers initiated from PVDF-I. The direct halide VDF initiation, VDF-CRP, and the complete halide chain-end activations open up novel synthetic avenues for the photomediated synthesis of architecturally complex fluoromaterials. Thus, main-chain fluorinated polymers can be grafted or block copolymerized directly from any substrates containing suitable halide initiators, and conversely, the polymerization of other monomers can be initiated quantitatively from their chain ends. Using multifunctional initiators, the synthesis of star and hyperbranched systems can be envisioned as well. Lastly, the R_F-I/$Mn_2(CO)_{10}$ protocol may also be applicable in radical trifluoromethylation reactions, which are in great demand in organic chemistry.[32]

■ ASSOCIATED CONTENT

Supporting Information

Materials, techniques, experimental procedures, initiator chart, ^{1}H and ^{19}F NMR and IR spectra and discussions, tables with full characterization of all homo- and copolymerizations (including initiator and solvent effect), kinetics, and dependence of the iodine chain ends on conversion. This material is available free of charge via the Internet at http://pubs.acs.org.

■ AUTHOR INFORMATION

Corresponding Author

asandei@ims.uconn.edu

Notes

The authors declare no competing financial interest.

■ ACKNOWLEDGMENTS

The University of Connecticut is acknowledged for support.

■ REFERENCES

(1) (a) Ameduri, B. *Macromolecules* **2010**, *43*, 10163. (b) Ameduri, B. *Chem. Rev.* **2009**, *109*, 6632. (c) Ameduri, B.; Boutevin, B. *Well Architectured Fluoropolymers: Synthesis, Properties and Applications*; Elsevier: Amsterdam, 2004; pp 1−99. (d) Hansen, N. M. L.; Jankova, K.; Hvilsted, S. *Eur. Polym. J.* **2007**, *43*, 255.

(2) Braunecker, W.; Matyjaszewski, K. *Prog. Polym. Sci.* **2007**, *32*, 93.

(3) Goto, A.; Fukuda, T. *Prog. Polym. Sci.* **2004**, *29*, 329.

(4) (a) Boutevin, B. *J. Polym. Sci., Part A: Polym. Chem.* **2000**, *38*, 3235. (b) Ameduri, B.; Boutevin, B. *Top. Curr. Chem.* **1997**, *192*, 165.

(5) David, G.; Boyer, C.; Tonnar, J.; Ameduri, B.; Lacroix-Desmazes, P.; Boutevin, B. *Chem. Rev.* **2006**, *106*, 3936.

(6) Ameduri, B.; Ladavière, C.; Delolme, F.; Boutevin, B. *Macromolecules* **2004**, *37*, 7602.

(7) Boyer, C.; Valade, D.; Sauguet, L.; Ameduri, B.; Boutevin, B. *Macromolecules* **2005**, *38*, 10353.

(8) Boyer, C.; David, V.; Lacroix-Desmazes, P.; Ameduri, B.; Boutevin, B. *J. Polym. Sci., Part A: Polym. Chem.* **2006**, *44*, 5763.

(9) Valade, D.; Boyer, C.; Ameduri, B.; Boutevin, B. *Macromolecules* **2006**, *39*, 8639.

(10) (a) Oka, M.; Tatemoto, M. In *Contemporary Topics in Polymer Science*; Bailey, W. J., Tsuruta, T., Eds.; Plenum Press: New York, 1984; Vol. 4, pp 763−781. (b) Tatemoto, M. In *Polymeric Materials Encyclopedia*; Salamone, J. C., Ed.; CRC Press: Boca Raton, FL, 1996; Vol. 5, pp 3847−3862.

(11) (a) Fukuda, T.; Goto, A.; Tsujii, Y. In *Handbook of Radical Polymerization*; Matyjaszewski, K., Davis, T. P., Eds.; Wiley: New York, 2002; pp 407−462. (b) Gaynor, S. G.; Wang, J. S.; Matyjaszewski, K. *Macromolecules* **1995**, *28*, 8051.

(12) (a) Chen, Q. Y.; Yang, Z. Y. *J. Fluorine Chem.* **1985**, *28*, 399. (b) Chen, M. Y.; Yang, Z. Y.; Zhao, C. X.; Qiu, Z. M. *J. Chem. Soc., Perkin Trans. 1* **1988**, *3*, 563. (c) Hu, C. M.; Qiu, Y. L. *J. Chem. Soc., Perkin Trans. 1* **1992**, *13*, 1569.

(13) Zhang, Z. C.; Chung, T. C. *Macromolecules* **2006**, *39*, 5187.

(14) Balague, J.; Ameduri, B.; Boutevin, B.; Caporiccio, G. *J. Fluorine Chem.* **1995**, *70*, 215.

(15) (a) Haszeldine, R. N.; Steele, B. R. *J. Chem. Soc.* **1954**, 923. (b) Saint-Loup, R.; Ameduri, B. *J. Fluorine Chem.* **2002**, *116*, 27. (c) Ameduri, B.; Billard, T.; Langlois, B. *J. Polym. Sci., Part A: Polym. Chem.* **2002**, *40*, 4538.

(16) (a) Rowlands, G. J. *Tetrahedron* **2009**, *65*, 8603. (b) Gilbert, B. C.; Parsons, A. F. *J. Chem. Soc., Perkin Trans. 2* **2002**, *3*, 367. (c) Gilbert, B.; Kalz, W.; Lindsay, C. I.; McGrail, P. T.; Parsons, A. F.; Whittaker, D. T. *J. Chem. Soc., Perkin Trans. 1* **2000**, 1187.

(17) (a) Brimm, E. O.; Lynch, M. A. Jr.; Sesny, W. J *J. Am. Chem. Soc.* **1954**, *76*, 3831. (b) Goodman, J.; Peters, K.; Vaida, V. *Organometallics* **1986**, *5*, 815.

(18) (a) Sarakha, M.; Ferraudi, G. *Inorg. Chem.* **1999**, *38*, 4605. (b) Hughey, J. L.; Anderson, C. P.; Meyer, T. J. *J. Organomet. Chem.* **1977**, *125*, C49.

(19) Haines, L. I. B.; Poe, A. J. *Nature* **1968**, *215*, 699.

(20) (a) Gilbert, B.; Harrison, R.; Lindsay, C.; McGrail, P.; Parsons, A. F.; Southward, R.; Irvine, D. J. *Macromolecules* **2003**, *36*, 9020. (b) Jenkins, D. W.; Hudson, S. M. *Macromolecules* **2002**, *35*, 3413. (c) Acik, G.; Kahveci, M.; Yagci, Y. *Macromolecules* **2010**, *43*, 9198.

(21) (a) Koumura, K.; Satoh, K.; Kamigaito, M. *Macromolecules* **2008**, *41*, 7359. (b) Koumura, K.; Satoh, K.; Kamigaito, M. *J. Polym. Sci., Part A: Polym. Chem.* **2009**, *47*, 1343. (c) Koumura, K.; Satoh, K.; Kamigaito, M. *Macromolecules* **2009**, *42*, 2497.

(22) (a) Doll, W. W.; Lando, J. B. *J. Appl. Polym. Sci.* **1970**, *14*, 1767. (b) Russo, S.; Behari, K.; Chengji, S.; Pianca, M.; Barchiesi, E.; Moggi, G. *Polymer* **1993**, *22*, 4777.

(23) (a) Galin, J.; Lutringer, G.; Galin, M. *J. Appl. Polym. Sci.* **1989**, *37*, 487. (b) Tundo, Y.; Selva, M. *Acc. Chem. Res.* **2002**, *35*, 706. (c) Odian, G. *Principles of Polymerization*, 4th ed.; Wiley: New York, 2004; pp 292−298.

(24) Gordon, A .S.; Norris, W. P. *J. Phys. Chem.* **1965**, *69*, 3013.

(25) (a) Burchill, M. T. *Prog. Batteries Battery Mater.* **1998**, *17*, 144. (b) Saunier, J.; Alloin, F.; Sanchez, J. Y.; Barriere, B. *J. Polym. Sci., Part B: Polym. Phys.* **2004**, *42*, 532.

(26) (a) Drago, R. S.; Wong, N. M.; Ferris, D. C. *J. Am. Chem. Soc.* **1992**, *114*, 91. (b) Friestad, G. K.; Marie, J. C.; Suh, Y. S.; Qin, J. *J. Org. Chem.* **2006**, *71*, 7016.

(27) (a) Pan, X.; Philbin, C. E.; Castellani, M. P.; Tyler, D. R. *Inorg. Chem.* **1988**, *27*, 671. (b) Martinho Simoes, J. A.; Beauchamp, J. L. *Chem. Rev.* **1990**, *90*, 629.

(28) Okafo, E. N.; Whittle, E. *Int. J. Chem. Kinet.* **1975**, *7*, 287.

(29) (a) Balague, J.; Ameduri, B.; Boutevin, B.; Caporiccio, G. *J. Fluorine Chem.* **2000**, *102*, 253. (b) Ameduri, B.; Boutevin, B. *J. Fluorine. Chem.* **1999**, *100*, 97. (c) Vukicevic, R.; Beuermann, S. *Macromolecules* **2011**, *44*, 2597. (d) Jol, S. M.; Lee, W. S.; Ahn, B. S.; Park, K. Y.; Kim, K. A.; Paeng, I. R. *Polym. Bull.* **2000**, *44*, 1.

(30) Fulmer, G.; Miller, A.; Sherden, N.; Gottlieb, H.; Nudelman, A.; Stoltz, B.; Bercaw, J.; Goldberg, K. *Organometallics* **2010**, *29*, 2176.

(31) (a) Herman; Uno, T.; Kubono, A.; Umemoto, S.; Kikutani, T.; Okui, N. *Polymer* **1997**, *38*, 1677. (b) Ferguson, R. C.; Brame, E. G. *J. Phys. Chem.* **1979**, *83*, 1397. (c) Guiot, J.; Ameduri, B.; Boutevin, B. *Macromolecules* **2002**, *35*, 8694. (d) Pianca, M.; Barchiesi, E.; Esposto, G.; Radice, S. *J. Fluorine Chem.* **1999**, *95*, 71. (e) Wormald, P.; Ameduri, B.; Harris, R. K.; Hazendonk, P. *Polymer* **2008**, *49*, 3629. (f) Duc, M.; Ameduri, B.; Boutevin, B.; Kharrouni, M.; Sage, J. M. *Macromol. Rapid Commun.* **1998**, *199*, 1271.

(32) Nagib, D. A.; MacMillan, D. W. *Nature* **2011**, *224*, 224.

Mild Temperature $Mn_2(CO)_{10}$-Photomediated Controlled Radical Polymerization of Vinylidene Fluoride and Synthesis of Well Defined PVDF Block Copolymers

Alexandru D. Asandei*, Olumide Adebolu and Christopher P. Simpson

University of Connecticut, Institute of Materials Science and Department of Chemistry. 97 N. Eagleville Rd., Storrs, CT. 06069-3136.

asandei@ims.uconn.edu

Supporting Information

Experimental

Materials. Manganese carbonyl ($Mn_2(CO)_{10}$, (Strem chemicals, 98%), vinylidene fluoride (VDF,99.9%), 2-Iodoheptafluoropropane (PFIPI, 97%)), 1-iodononafluorobutane (perfluorobutyl iodide, PFBI, 98%), ethyl bromodifluoroacetate (EBDFA, 99%), 1,1,2-trichlorotrifluoroethane (TCTFE, 99%), 1,1,1,3,3-Pentafluorobutane (99%), 3-Iodo-1,1,2,2-tetrafluoropropane (98%), 1,8-dichloroperfluorooctane (99%), iodotrifluoromethane (CF_3I, 99%), 1,6-diiododododecafluorohexane (98%), 1,2-dichloro-1,1,2-trifluoro-2-iodoethane (90+%), hexafluorobenzene (HFBz, 99+%), 1,4-dibromoooctafluorobutane (98%), hexafluoropropene (HFP, 99%), chlorotrifluoroethylene (CTFE, 99%), bromotrifluoroethylene (BTFE, 98%), vinyl fluoride (VF, 98%), trifluorometyl trifluorovinyl ether (99%), 1-Chloro-1-fluoroethylene (98%), 1,1-dichloro-2,2-difluoroethylene (90 %) (all from Synquest), ethyl iododifluoroacetate (EIDFA, 97%), heptafluorobenzyl iodide (97%), iodoperfluoro-tert-butane (97%), 1,2-Diiodotetrafluoroethane (97%) (All from Matrix Scientific); 1,3-dibromo-1,1,3,3-tetrafluoropropane (97%), carbon tetrabromide (CBr_4, 98%) (both from Alfa Aesar), heptafluorobutyryl chloride (98%), 1,4-diiodoperfluorobutane(98%), chloroform ($CHCl_3$, stabilized with ca. 1% ethanol), 4-methoxybenzenesulfonyl chloride (MBSC, 99%), iodoform (CHI_3 99+%), dimethyl sulfoxide (DMSO, 99.8%), 4-iodoanisole(98%), ethyl 2-bromoisobutyrate (EBIB, 98%), thymol iodide, 1,4-dioxane (Diox, 99.7%), N,N'-dimethylacetamide, (DMAc, 99%), ethylene carbonate (EC, +99%), ε-caprolactone (CL, 99%), benzonitrile (BN, 99%, extra pure), 4-methyl-2-pentanone (reagent ACS), isopropanol (99.5%), vinyl acetate (VAc, 99+%), acrylonitrile (99+%), styrene (99%), methyl acrylate (MA, 99%) (all from Acros Organics); iodomethane (CH_3I, ReagentPlus, 99.5%), bromotrichloromethane ($BrCCl_3$, 99%), 1-Iodohexane (98+%), halocarbon oil 27, methanesolfonyl chloride (≥99.7%) ,

N-iodosuccinimide (NIS, 95%), hexachloroethane (99%), trifluoromethanesulfonyl chloride (≥99%), α,α,α-trifluorotoluene (TFT, 99%), bromoform ($CHBr_3$, ≥99%), acetonitrile (ACN, 99%), iodoacetonitrile (98%), 1H,1H,7H-dodecafluoroheptyl acrylate (95%), 2-bromopropionitrile (97%), dimethyl carbonate (DMC, ≥ 99% anhydrous), 2-butanone(ACS reagent, ≥99%), trimethyl phosphate (TMP, 99+%), diethyl carbonate (DEC, ≥99%), β-butyrolactone(98+%), γ-butyrolactone (ReagentPlus, ≥99%), propylene carbonate (PC, 99.7%, HPLC grade), methanol (99%), anisole (99.7%), tert-butanol (anhydrous, 99.5%), dichloromethane (anhydrous, > 99.5%), 1,2-dichloroethane (anhydrous, 99.8%), o-cresol (99%), ethyl acetate (anhydrous, 99.8%), cyclopentanone (99%), allyl iodide (98%), 1,1,1,3,3,3-hexafluoro-2-propanol (HFIPA, > 99%), (1-bromoethyl)benzene (BEB, 97%), 2-iodo-2-methylpropane (copper-stabilized, 95%), diethylene glycol dimethyl ether (diglyme, anhydrous 99.5%), and carbon tetraiodide (97 %), 1,3-butadiene (≥99%) (all from Aldrich); allyl bromide (>98%), α,α'-dibromo-p-xylene (DBPX, ≥98%), tetramethylurea (≥99.0%), N-bromosuccinimide (NBS, >95%), poly(ethylene oxide) 2000, vinyl chloride (≥99.5%) (all from Fluka); δ-valerolactone (99%) 1,10-diiododecane (97%), di-tert-butyldicarbonate (99%), allyl chloride (98%), (all from Janssen Chimica); carbon tetrachloride (CCl_4,), acetic anhydride (certified A.C.S.), N,N'-Dimethylformamide (DMF, 99.9%), trifluoroacetic anhydride (reagent grade), diethylene glycol monoethyl ether (lab grade), diethylether (anhydrous, 99%), (all from Fisher Scientific); acetone-d_6 (Cambridge Isotope Laboratories, Inc., D, 99.9%), tetrahydrofuran (THF, 99%, acetone, 99.9 % both J. T. Baker) were used as received. Ethyl-2-iodoisobutyrate (EIIB), α,α'-diiodo-*p*-xylene (DIPX) and $Mn(CO)_5$-I were prepared from ethyl-2-bromoisobutyrate (EBIB, 98%, Acros), α,α'-dibromo-*p*-xylene, (DBPX, ≥98%, Fisher)[1] (99%, Fisher) and respectively from $Mn_2(CO)_{10}$[2] as described in the literature.

Techniques. ^{1}H NMR (500 MHz) and ^{19}F-NMR (400 MHz) spectra were recorded on a Bruker DRX-500 and respectively on a Bruker DRX-400 at 24 ^{0}C in acetone-d_6. IR spectra were recorded on a Nicholet 560 spectrometer on KBr plates or pellets. GPC analyses were performed on a Waters gel permeation chromatograph equipped with a Waters 2414 differential refractometer and a Jordi 2 mixed bed columns setup at 80^{0}C. DMAc (Fisher, 99.9% HPLC grade) was used as eluent at a flow rate of 1 mL/min. Number-average (M_n) and weight-average molecular weights (M_w) were determined from calibration plots constructed with polymethylmethacrylate standards. All reported polydispersities are those of water precipitated samples. While narrower PDIs could be obtained by MeOH precipitation, this may also lead to partial fractionation, especially for lower molecular weight samples.

Polymerizations

PVDF Homopolymerization: In a typical reaction, a 35-mL Ace Glass 8648 # 15 Ace-Thread pressure tube equipped with a bushing, and plunger valve with two O-rings and containing a magnetic stir bar, $Mn_2(CO)_{10}$, (53.6 mg, 0.14 mmol) and solvent (*e.g.* DMC, 3 mL) was degassed with He and placed in a liquid nitrogen bath. Note that it is important to use He for degassing, as N_2 or Ar would actually condense in the tube in a liquid nitrogen bath. The tube was subsequently opened, and the initiator (*e.g.* CF_3-$(CF_2)_3$-I (PFBI), 0.12 mL, 0.69 mmol) was added, followed by the condensation of VDF (1.1 g, 17.2 mmol), directly into the tube, which was then re-degassed with He. The amount of condensed VDF was determined by weighing the closed tube before and after the addition of the monomer. The tube was then placed in behind a plastic shield, in a thermostated oil bath illuminated with a commercial GE Helical 26 W fluorescent white light Hg spiral bulb, from about 2-4 cm (see Figure S1). For polymerization kinetics, identical reactions were set up simultaneously and stopped at different polymerization

times. At the end of the reaction, the tube was carefully placed in liquid nitrogen, slowly opened behind the shield, and allowed to thaw to room temperature in the hood, with the concomitant release of unreacted VDF. The contents were poured in water, filtered and dried. The polymer was than dissolved in DMAC, and the residual Mn inorganics (which may interfere with the NMR signals) were removed by column chromatography. The polymer was finally reprecipitated in water, filtered and dried. While precipitation in MeOH is feasible, it will also lead to fractionation and narrowing of the polydispersity by about 0.2, especially on lower molecular weight samples. Thus, all reported GPC results are from water precipitation. The monomer conversion was determined as the ratio of the differences of the tube weight before and after the reaction and respectively before and after VDF charging (*i.e.* c = ($Wt_{\text{after VDF condensation}}$ - $Wt_{\text{after VDF release}}$)/($Wt_{\text{after VDF condensation}}$ –$Wt_{\text{before VDF addition}}$), as well as the ratio of the dry polymer to the condensed VDF. Both procedures gave conversions within < 5% of each other. In this particular example the reaction time was 16 h, Mn = 4,015, Mw/Mn =1.31.

Synthesis of Poly(VDF-*co*-HFP) Random Copolymers

An identical setup was used, except VDF (2.2 g, 34 mmol) was first condensed in the tube, followed by HFP (1.3 g, 8.6 mmol). The tube was degassed and the polymerization was carried out 40 °C under visible light irradiation. After a given amount of time, the solution was precipitated in cold hexane, filtered and dried. M_n = 2,764 PDI = 1.85 conversion = 56%, corresponding to the third point in the kinetic in Figure S3.

Synthesis of PVDF Block Copolymers. An example of the block synthesis is as follows: A Schlenk tube containing a DMAC solution of PVDF-I or I-PVDF-I (in this case, I-PVDF-I, M_n = 2,500, PDI = 1.34, with a total halide chain end functionality of F = 95% ($F_{1,Pn\text{-}CH2\text{-}CF2\text{-}I}$ = 0.64 and $F_{2,Pm\text{-}CF2\text{-}CH2\text{-}I}$ = 0.31, 100 mg, 0.05 mmol in 2 mL of DMAC), a second

monomer (*e.g.* styrene, 215 mg, 2.1 mmol) and $Mn_2(CO)_{10}$ (36 mg, 0.1 mmol) was degassed under Ar then heated to 110 ^oC under visible light irradiation for 5 h. The solution was precipitated in MeOH, filtered and dried. M_n = 14,500, PDI = 2.25 conv. = 67%, and composition, VDF/St = 30/70.

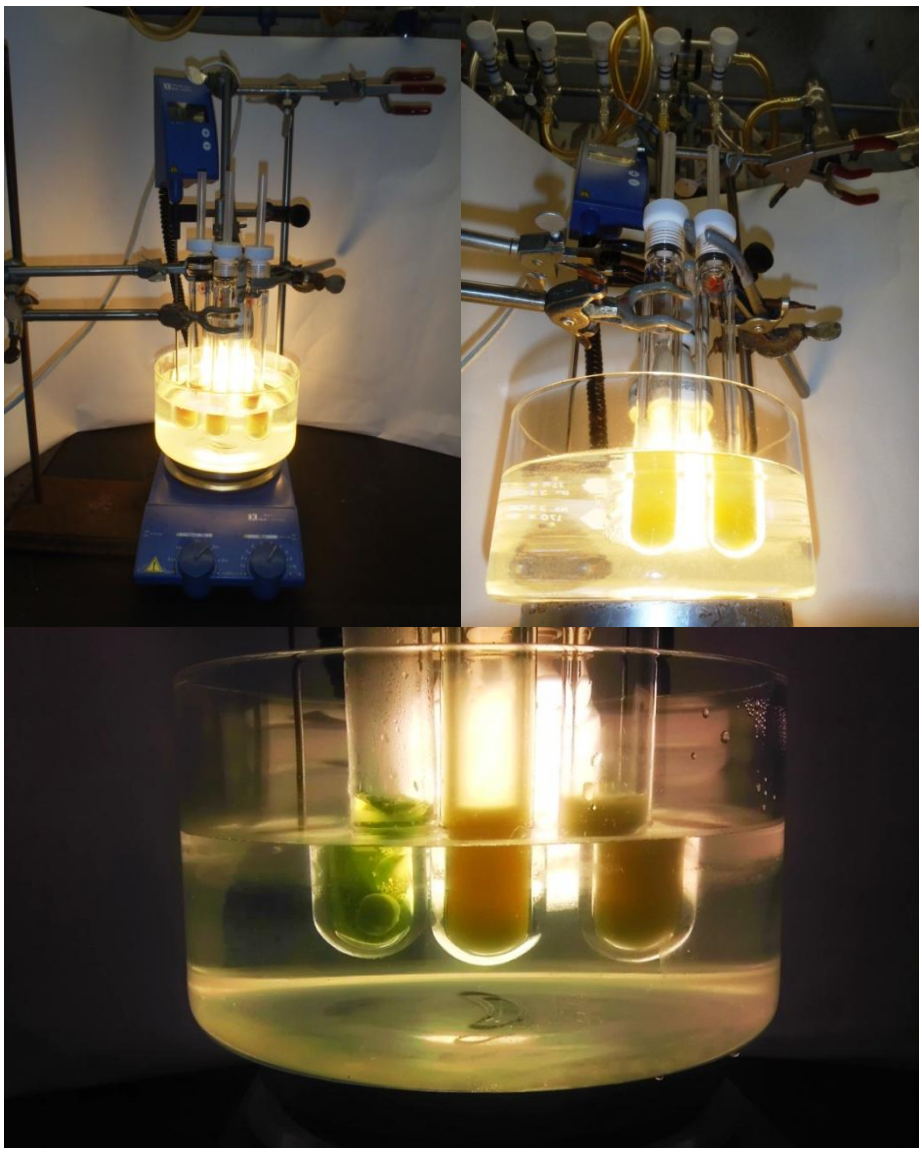

Figure S1. $Mn_2(CO)_{10}$ mediated VDF photopolymerization typical setup (top), and the polymerization at several stages of conversion (bottom).

CHART S1. Halide substrates tested as initiators for $Mn_2(CO)_{10}$ mediated VDF photopolymerizations. The compounds are qualitatively arranged by structure (rows) and halide type (columns), where color (Cl = blue, Br = green, Iodine = red) also indicates successful addition to VDF. (R_F= CF_3-$(CF_2)_n$- or -$(CF_2)_n$-).

Structure/ Functionality	Chloride	Bromide	Iodide
R-X	-	-	CH_3I, CH_3-$(CH_2)_5$-I
X-R-X	-	-	I-$(CH_2)_{10}$-I
CH_2=CH-CH_2-X	CH_2=CH-CH_2-Cl	-	CH_2=CH-CH_2-I
NC-CH(R)-X	-	NC-$CH(CH_3)$-Br	NC-CH_2-I
$(CH_2$-$CO)_2$N-X	-	Br-N$(CO$-$CH_2)_2$	-
Ar-X	-	-	CH_3O-Ph-I
C_6H_5-$CH(CH_3)$-X	-	C_6H_5-$CH(CH_3)$-Br	-
$C_6H_4(CH_2$-$X)_2$	-	$C_6H_4(CH_2$-$Br)_2$	$C_6H_4(CH_2$-$I)_2$
C_6F_5-CF_2-X	-	-	C_6F_5-CF_2-I
$(CH_3)_2C(COOEt)$-X	-	$(CH_3)_2C(COOEt)$-Br	$(CH_3)_2C(COOEt)$-Br
$CF_2(COOEt)$-X	-	$CF_2(COOEt)$-Br	$CF_2(COOEt)$-I
CH_2X_2	CH_2Cl_2	-	CH_2I_2
X_2CH-CHX_2	Cl_2CH-$CHCl_2$	-	-
CHX_3	$CHCl_3$	$CHBr_3$	CHI_3
CCl_3-X	-	CCl_3-Br	-
X_3C-CX_3	Cl_3C-CCl_3	-	-
CX_4	CCl_4	CBr_4	Cl_4
R-SO_2-X	CH_3SO_2Cl	-	-
R_F-SO_2-X	CF_3SO_2Cl	-	-
Ar-SO_2-X	CH_3O-Ph-SO_2-Cl		-
R_F-CO-X	CF_3-CF_2-CF_2-CO-Cl	-	-
R_F-CH_2-X	-	-	H-CF_2-CF_2-CH_2-I
X-CF_2-CH_2-CF_2- X	-	Br-CF_2-CH_2-CF_2-Br	-
R_F-X	-	-	CF_3-I, CF_3-$(CF_2)_{1,3}$-I
X-R_F-Y	-	-	Cl-CF_2-$(CF_2)_4$-CF_2-I
X-R_F-X	Cl-CF_2-$(CF_2)_6$-CF_2-Cl	Br-CF_2-$(CF_2)_2$-CF_2-Br	I-CF_2-$(CF_2)_{2,4}$-CF_2-I
X-R_F-CFXY	-	-	Cl-CF_2-CFCl-I
X-R_F-CFX_2	Cl-CF_2-CFCl-Cl	-	-
X-$(R_F$-$CFX)_n$-X	Cl-$(CF_2$-$CFCl)_n$-Cl	-	-
$(CF_3)_2$CF-X	-	-	$(CF_3)_2$CF-I
$(CF_3)_3$C-X	-	-	$(CF_3)_3$C-I

Table S1. $Mn_2(CO)_{10}$ Mediated VDF Polymerizations: control experiments (exp. 1-4); temperature effect (exp. 5-16), initiator effect: good initiators (exp. 17-42), [VDF]/[I] ratio (exp 43-49), other monomers (exp. 50-52), and ineffective initiators (exp. 53-73).

Exp#	Initiator	Temp °C	[VDF]/[I]/ $[Mn_2(CO)_{10}]$	Time (Hrs)	Conv (%)	k_p^{app} (h^{-1})	Mn	PDI
1	-	40	25/0/0	63	0	-	-	-
2	-	40	25/0/0.2	64	0	-	-	-
3	CF_3-$(CF_2)_2$-CF_2-I	40	25/1/0	20	0	-	-	-
4	CF_3-$(CF_2)_2$-CF_2-I[a]	40	25/1/0.2	93	0	-	-	-
5	CF_3-$(CF_2)_2$-CF_2-I	40	25/1/0.2	22	81	0.074	1,700	1.41
6	CF_3-$(CF_2)_2$-CF_2-I	0	25/1/0.2	11	67	0.050	2,300	1.57
7	CF_3-$(CF_2)_2$-CF_2-I[b]	25	50/1/0.15	36	10	0.002	1,000	1.33
8	CF_3-$(CF_2)_2$-CF_2-I[b]	40	25/1/0.15	96	16	0.002	1,900	1.26
9	CF_3-$(CF_2)_2$-CF_2-I	40	25/1/0.2	22	87	0.094	2,300	1.49
10	I-CF_2-$(CF_2)_4$-CF_2-I	40	50/1/0.1	33	42	0.017	2,600	1.34
11	CF_3-$(CF_2)_2$-CF_2-I	40	50/1/0.2	18	65	0.058	3,100	1.79
12	CF_3-$(CF_2)_2$-CF_2-I[b]	40	50/1/0.15	64	23	0.004	1,400	1.29
13	I-CF_2-$(CF_2)_4$-CF_2-I	65	50/1/0.1	14	58	0.062	2,400	1.42
14	CF_3-$(CF_2)_2$-CF_2-I	75	50/1/0.2	4	60	0.223	2,000	1.55
15	CF_3-$(CF_2)_2$-CF_2-I[b]	80	25/1/0.15	24	40	0.021	1,000	1.28
16	CF_3-$(CF_2)_2$-CF_2-I[b]	100	50/1/0.15	27	40	0.019	900	1.32
17	CF_3SO_2Cl[b]	40	20/1/0.1	75	10	0.001	600	1.85
18	$CHCl_3$	40	50/1/0.2	63	20	0.004	13,300	1.65
19	CCl_3Br	40	25/1/0.2	64	34	0.007	2,500	2.09
20	Cl_3C-CCl_3	40	25/1/0.2	68	71	0.018	5,000	1.86
21	CCl_4	40	25/1/0.5	17	56	0.050	5,000	1.36
22	CF_3-$(CF_2)_2$-CO-Cl	40	50/1/0.2	62	11	0.002	7,400	2.03
23	Cl-FClC-CF_2-Cl	40	50/1/0.2	10	53	0.079	7,300	2.17
24	Cl-$(CF_2$-$CFCl)_{3\text{-}6}$-Cl	40	50/1/0.5	21	56	0.039	10,500	1.80
25	Cl-$(CF_2)_8$-Cl	40	25/1/0.25	40	19	0.005	9,300	1.74
26	Br-CF_2-CH_2-CF_2-Br	40	50/1/0.15	37	40	0.014	4,100	2.31
27	EtOOC-CF_2-Br	40	30/1/0.25	44	24	0.006	3,400	1.94
28	Br-$(CF_2)_4$-Br[b]	40	20/1/0.4	5	84	0.367	2,700	2.69
29	CH_3I	40	50/1/0.5	21	42	0.026	6,300	1.83
30	CH_3-$(CH_2)_5$-I	40	25/1/0.5	63	24	0.004	3,100	2.06
31	I-CH_2-$(CH_2)_8$-CH_2-I	40	50/1/0.8	120	28	0.003	11,000	2.43
32	HCF_2-CF_2-CH_2-I	40	100/1/0.5	16	49	0.042	4,400	1.88
33	EtOOC-CF_2-I	40	25/1/0.2	62	84	0.030	1,200	1.71
34	C_6F_5-CF_2-I	40	50/1/0.75	70	50	0.010	2,600	2.43
35	CF_3I[b]	40	50/10/0.2	42	30	0.008	1,400	1.21
36	CF_3-CF_2-I[b]	40	50/1/0.1	24	16	0.007	1,500	1.27
37	$(CF_3)_2CF$-I[b]	40	50/1/0.5	20	44	0.029	3,600	1.60
38	$(CF_3)_3C$-I	40	25/1/0.2	85	59	0.010	2,500	1.88
39	Cl-CF_2-CFCl-I	40	25/1/0.2	14	88	0.153	1,900	1.72
40	Cl-CF_2-$(CF_2)_4$-CF_2-I[b]	40	50/1/0.3	40	58	0.22	1,400	1.56

VDF/DMC = 1.1 g/3mL, unless otherwise noted. [a]Dark conditions, [b]ACN.

Table S1, Continued. $Mn_2(CO)_{10}$ Mediated VDF Polymerizations: control experiments (exp. 1-4); temperature effect (exp. 5-16), initiator effect: good initiators (exp. 17-42), [VDF]/[I] ratio (exp 43-52), other monomers (exp. 53-59), and ineffective initiators (exp. 60-80).

Exp#	Initiator	Temp °C	[VDF]/[I]/ $[Mn_2(CO)_{10}]$	Time (Hrs)	Conv (%)	k_p^{app} (h^{-1})	Mn	PDI
41	I-CF_2-$(CF_2)_2$-CF_2-I	40	25/1/0.4	6	87	0.340	1,900	1.68
42	I-CF_2-$(CF_2)_4$-CF_2-I	40	50/1/0.4	8	78	0.189	3,200	1.50
43	I-CF_2-$(CF_2)_4$-CF_2-I	40	25/1/0.1	8	86	0.246	1,700	1.24
44	I-CF_2-$(CF_2)_4$-CF_2-I	40	50/1/0.1	15	68	0.076	3,900	1.42
45	I-CF_2-$(CF_2)_4$-CF_2-I [c]	40	100/1/0.1	12	72	0.106	6,600	1.53
46	I-CF_2-$(CF_2)_4$-CF_2-I [d]	40	200/1/0.4	1.5	32	0.257	7,400	1.32
47	I-CF_2-$(CF_2)_4$-CF_2-I [d]	40	500/1/0.4	16	38	0.026	13,200	1.58
48	I-CF_2-$(CF_2)_4$-CF_2-I [c]	40	1000/1/0.2	20	37	0.028	21,200	1.60
49	I-CF_2-$(CF_2)_4$-CF_2-I [c]	40	5000/1/0.4	28	11	0.001	23,100	1.75
50	I-CF_2-$(CF_2)_4$-CF_2-I [c]	40	10,000/1/2	72	<3	-	29,500	1.99
51	I-CF_2-$(CF_2)_4$-CF_2-I [c]	40	50,000/1/2	72	<3	-	37,000	1.79
52	I-CF_2-$(CF_2)_4$-CF_2-I [c]	40	100,000/1/2	72	<3	-	51,500	1.62
53	CF_3-$(CF_2)_2$-CF_2-I [e]	40	25/1/0.2	18	59	0.050	1,900	1.24
54	CF_3-$(CF_2)_2$-CF_2-I [f]	40	50/1/1	40	10	0.003	6,200	1.71
55	CF_3-$(CF_2)_2$-CF_2-I [g]	40	25/1/0.2	38	89	0.058	6,400	2.62
56	CF_3-$(CF_2)_2$-CF_2-I [h]	40	100/1/0.5	46	85	0.041	700	1.27
57	CF_3-$(CF_2)_2$-CF_2-I [i]	40	50/1/0.5	72	45	0.008	500	1.75
58	CF_3-$(CF_2)_2$-CF_2-I [j]	40	80/20/1/0.2	60	56	0.014	2,800	1.85
59	CF_3-$(CF_2)_2$-CF_2-I [k]	40	70/30/1/0.5	43	44	0.013	1,900	1.99
60	CH_3SO_2Cl	40	25/1/0.5	48	0	-	-	-
61	CH_3O-Ph-SO_2Cl	40	25/1/0.5	68	0	-	-	-
62	CH_2Cl_2	40	25/1/0.15	72	0	-	-	-
63	Cl_2HC-$CHCl_2$ [b]	40	25/1/0.5	96	0	-	-	-
64	CH_2I_2 [b]	40	50/1/0.5	40	0	-	-	-
65	CH_2I_2	40	25/1/0.15	72	0	-	-	-
66	$CHBr_3$	40	50/1/0.2	63	0	-	-	-
67	CHI_3	40	50/1/0.2	63	0	-	-	-
68	CBr_4	40	30/1/0.5	21	0	-	-	-
69	CI_4	40	50/1/0.5	24	0	-	-	-
70	CH_2=CH-CH_2-Cl	40	50/1/0.75	70	0	-	-	-
71	CH_2=CH-CH_2-I	40	50/1/0.75	70	0	-	-	-
72	CH_3-(Ph)CH-Br	40	25/1/0.5	24	0	-	-	-
73	$(CH_2$-$CO)_2$N-Br [b]	40	50/1/0.5	72	0	-	-	-
74	Br-CH_2-Ph-CH_2-Br [b]	40	50/1/0.15	26	0	-	-	-
75	I-CH_2-Ph-CH_2-I [b]	40	50/1/0.15	200	0	-	-	-
76	CH_3-CH(CN)-Br [b]	40	25/1/0.15	120	0	-	-	-
77	CN-CH_2-I	40	25/1/0.5	63	0	-	-	-
78	$(CH_3)_2$C(COOEt)-Br	40	25/1/0.5	85	0	-	-	-
79	$(CH_3)_2$C(COOEt)-I [b]	40	50/1/0.3	18	0	-	-	-
80	I-Ph-OCH_3	40	25/1/0.5	62	0	-	-	-

All experiments in DMC (VDF/DMC = 1.1 g/3mL), unless otherwise noted. [a]Dark conditions, [b]ACN. [c]VDF/DMC = 4.4 g/6mL. [d]VDF/DMC = 1.7 g/3mL, [e]CF_2=CFCl, [f]CF_2=CFBr, [g]CH_2=CFCl, [h]CCl_2=CF_2, [i]CH_2=CFH, [j]VDF/HFP, [k]VDF/CF_2=CF(OCF_3).

Table S2. Solvent Effect in $Mn_2(CO)_{10}$ Photomediated VDF Polymerizations.[a)]

Exp.	Solvent	Time (Hrs)	Conv (%)	k_p^{app} (h^{-1})	Mn	PDI
1	Anisole	63	0	-	-	-
2	Benzonitrile	24	0	-	-	-
3	Cyclopentanone	23	0	-	-	-
4	Diethylene glycol monoethyl ether	48	0	-	-	-
5	Diglyme	18	0	-	-	-
6	Dioxane	20	0	-	-	-
7	Diethyl ether	63	0	-	-	-
8	Isopropanol	18	0	-	-	-
9	*o*-Cresol	23	0	-	-	-
10	Tetramethylurea	48	0	-	-	-
11	Trifluorotoluene	56	0	-	-	-
12	THF	48	0	-	-	-
13	Trifluoroacetic anhydride	21	0	-	-	-
14	2-Butanone	72	10	0.001	1,700	1.12
15	DMF	74	13	0.002	2,800	1.15
16	4-Methyl-2-pentanone	72	15	0.002	1,500	1.12
17	DMSO	74	17	0.003	2,800	1.07
18	PEO M_n = 2000	63	15	0.003	1,000	1.19
19	DMAc	21	8	0.004	3,700	1.19
20	δ-Valerolactone	21	12	0.006	500	2.74
21	^{t}Bu-OH	17	10	0.006	600	1.29
22	Ethyl acetate	63	42	0.009	1,400	1.21
23	CH_2Cl_2	18	18	0.011	700	1.30
24	Acetic anhydride	48	42	0.011	1,000	1.21
25	γ-Butyrolactone	21	26	0.014	700	1.26
26	1,2-dichloroethane	20	27	0.016	800	1.47
27	Trimethylphosphate	16	21	0.015	3,200	1.18
28	Pentafluorobutane	20	26	0.015	1,000	1.48
29	MeOH	17	24	0.016	800	1.45
30	Hexafluorobenzene	14	21	0.017	600	1.39
31	Acetonitrile	22	41	0.024	1,200	1.35
32	β-Butyrolactone	21	40	0.024	1,000	1.39
33	ε-Caprolactone	21	40	0.024	1,100	1.28
34	H_2O	18	41	0.029	800	1.63
35	Diethyl carbonate	22	48	0.030	2,600	1.13
36	Propylene carbonate	17	43	0.033	800	1.41
37	Di^{t}butyldicarbonate	21	50	0.033	900	1.40
38	Ethylene carbonate	17	58	0.051	1,200	1.79
39	Heptafluoroisopropyl alcohol	23	78	0.066	1,400	1.37
40	Acetone	8	47	0.079	1,000	1.33
41	Dimethyl carbonate	16	84	0.114	4,000	1.31

[a)] $[VDF]/[CF_3\text{-}CF_2\text{-}CF_2\text{-}CF_2\text{-}I]/[Mn_2(CO)_{10}]$ = 25/1/0.2, T = 40 °C.

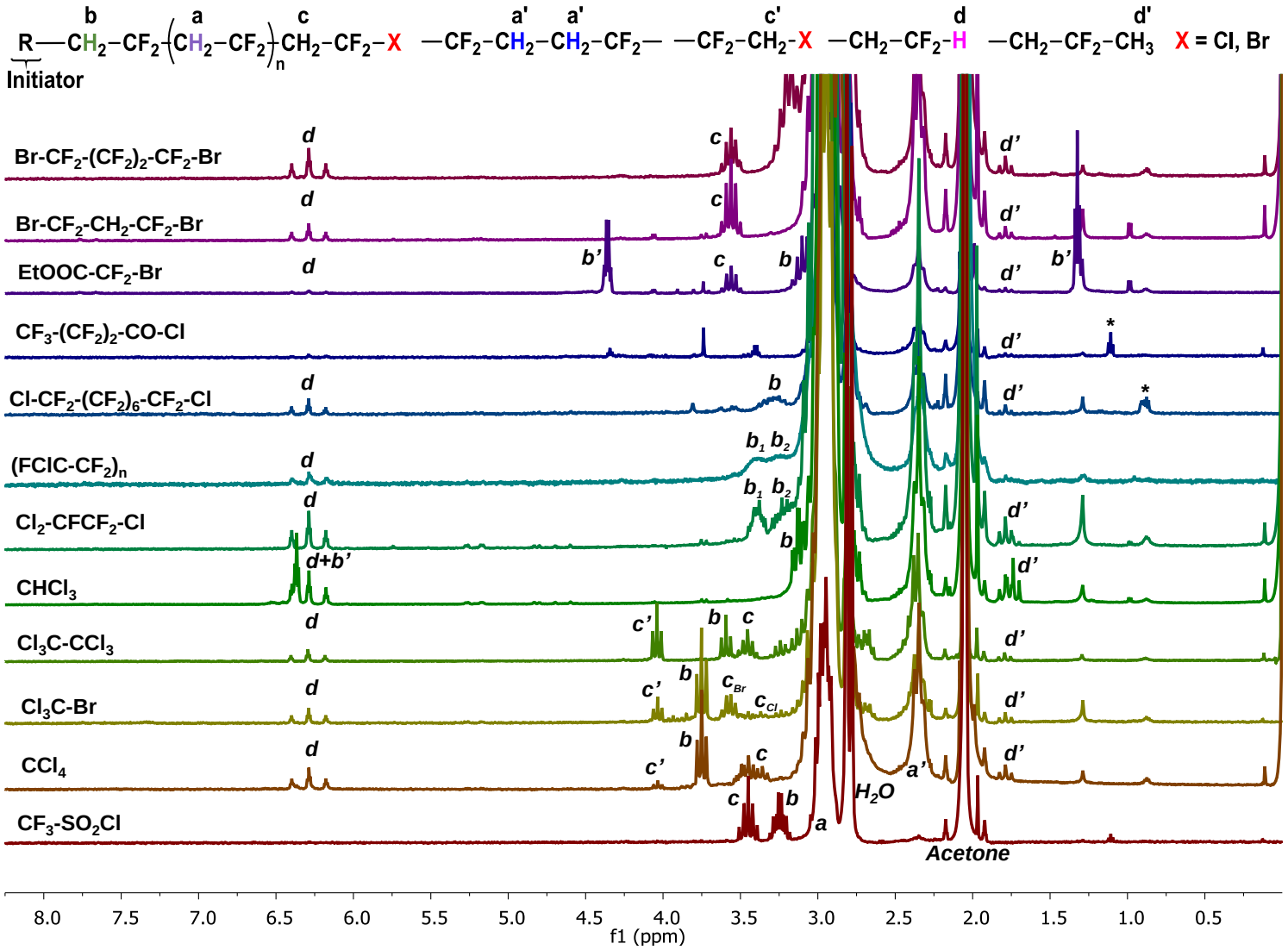

Figure S2a. 500 MHz acetone d_6 ^{1}H-NMR spectra of PVDF initiated from Cl and Br substrates. * Impurities associated with solvent or initiator.

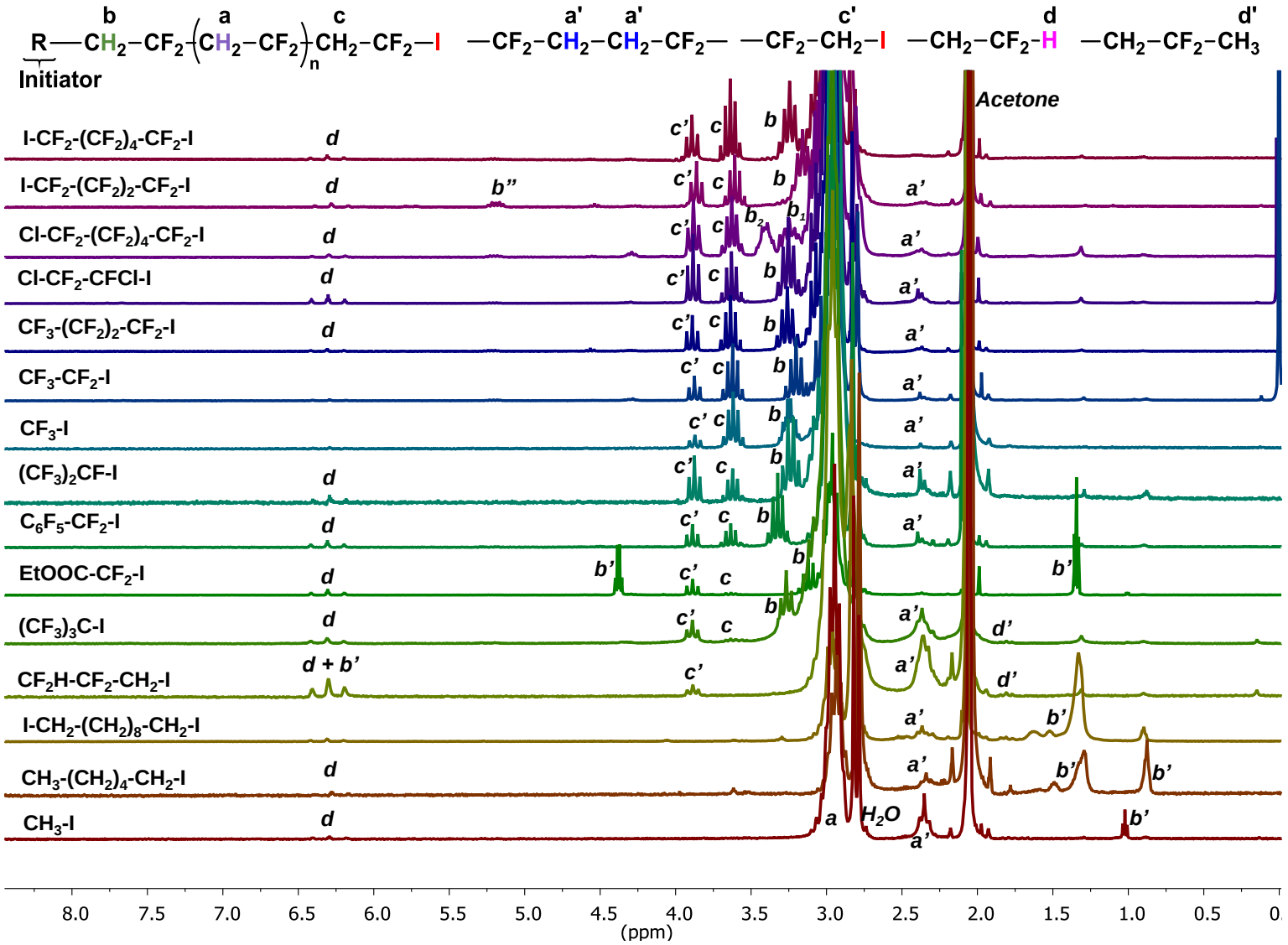

Figure S2b. 500 MHz acetone d_6 ^{1}H-NMR spectra of PVDF initiated from iodine substrates.

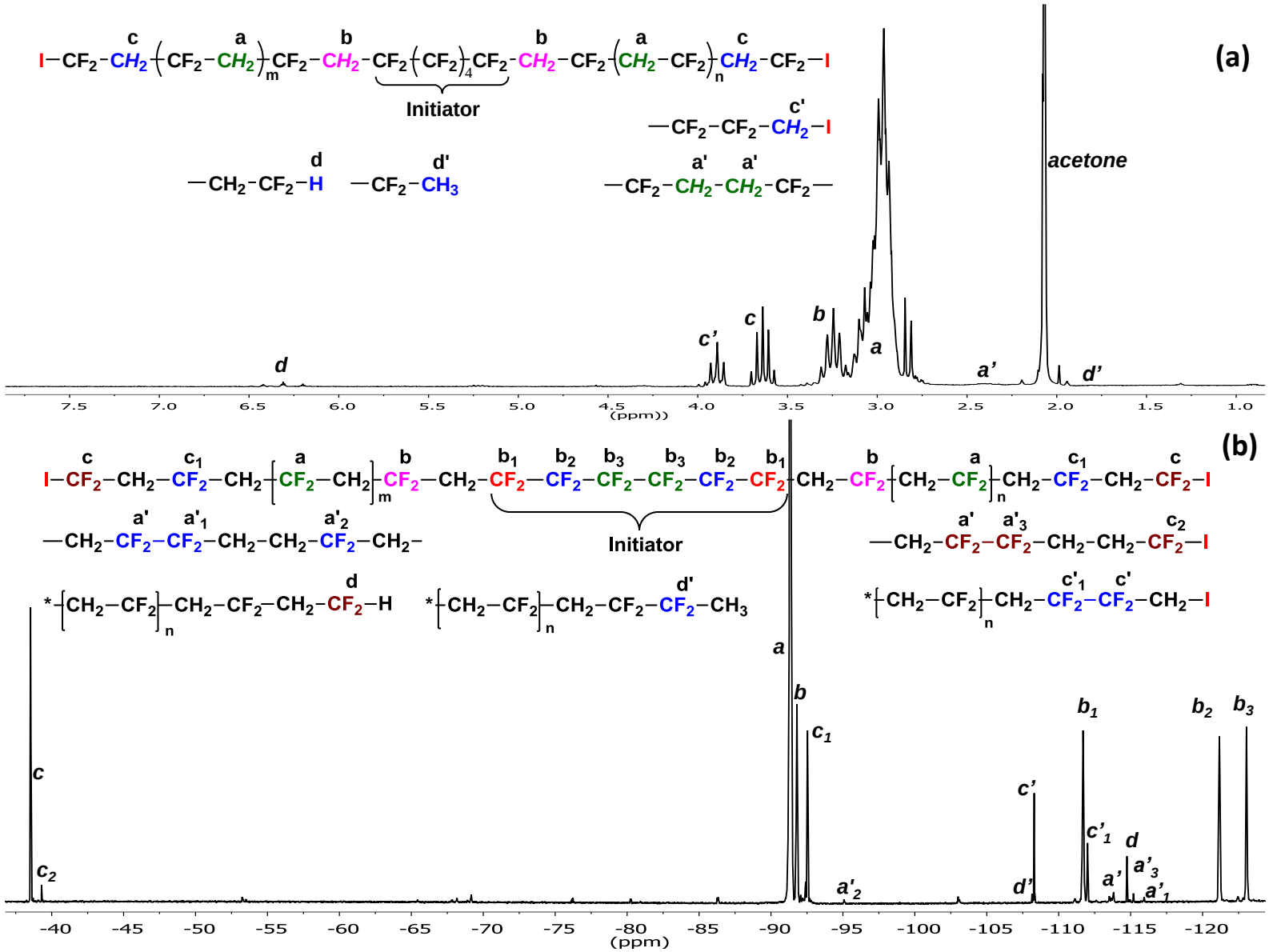

Figure S2c. Comparison of the ^{1}H and ^{19}F-NMR spectra of I-PVDF-I initiated from I-$(CF_2)_6$-I. [VDF]/[I-$(CF_2)_6$-I]/[$Mn_2(CO)_{10}$] = 50/1/0.1.

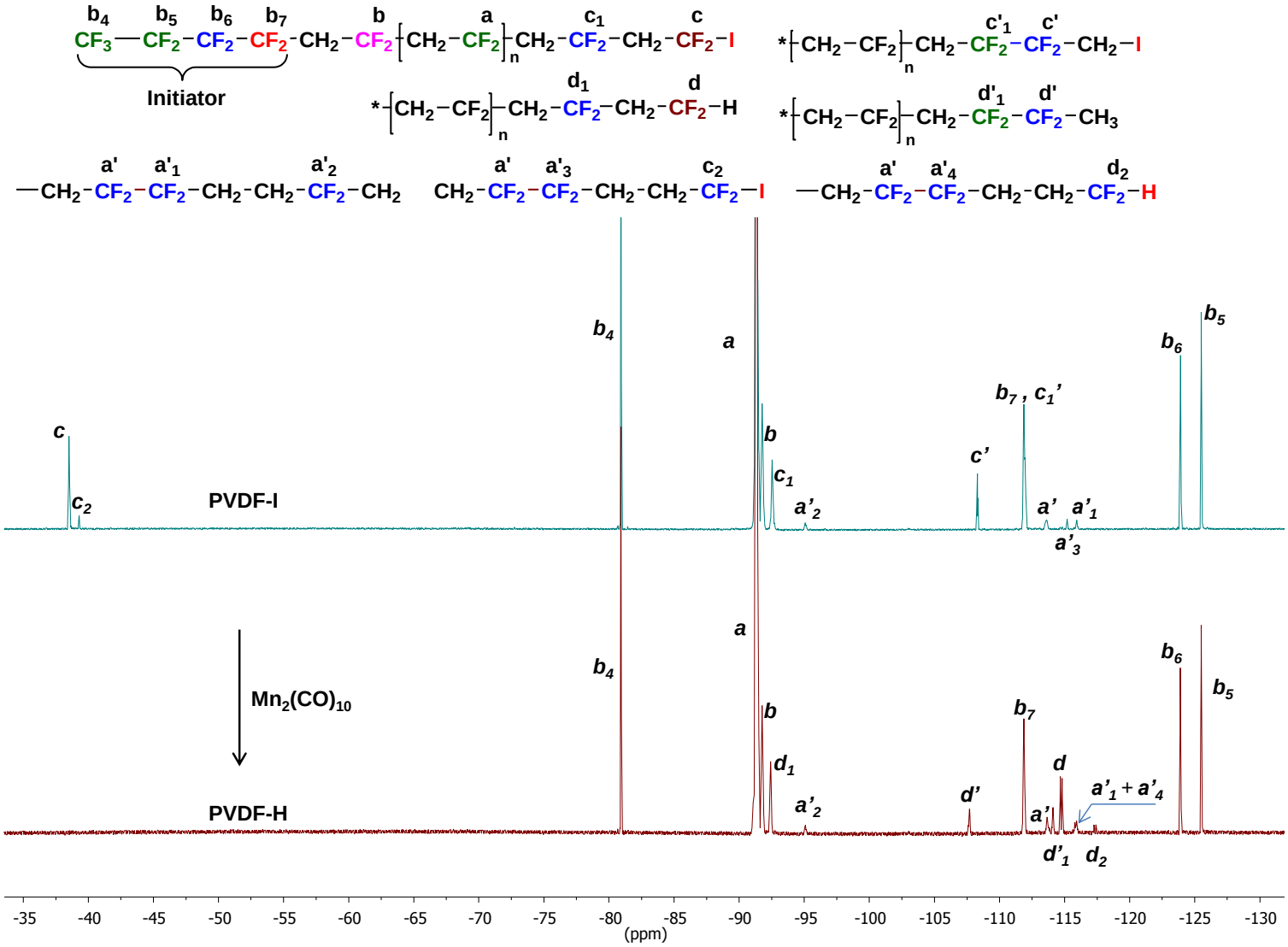

Figure S2d. Comparison of the ^{19}F-NMR spectra of PVDF-I initiated from CF_3-$(CF_2)_3$-I with the corresponding PVDF-H sample obtained after complete iodide abstraction by $Mn_2(CO)_{10}$.

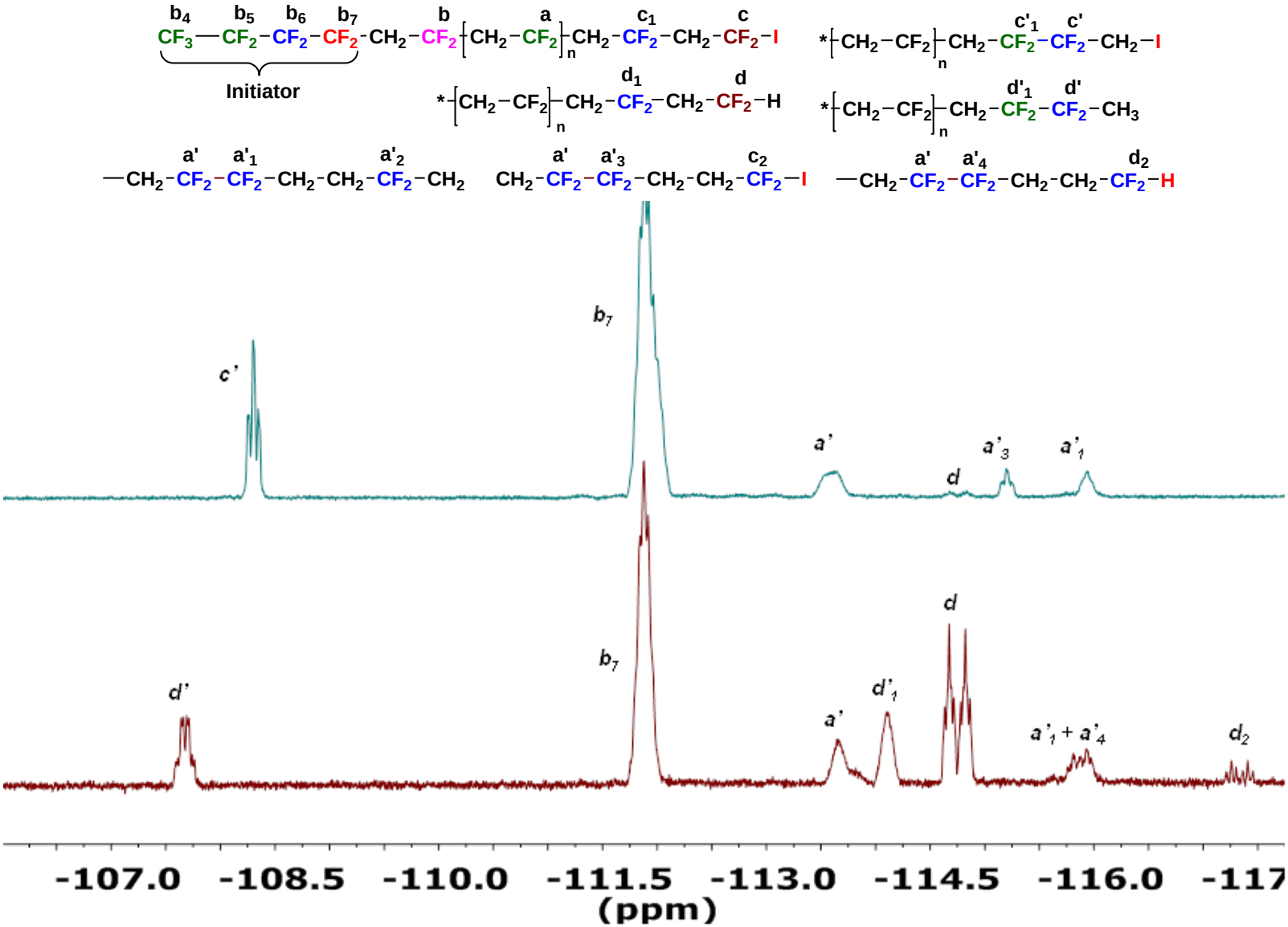

Figure S2e. Expansion of the -107 ppm to -117 ppm region from Figure S2d.

Table S3a. Characterization of PVDF samples initiated from Cl and Br substrates.

Expt #	Initiator	[VDF]/[I]/ $[Mn_2(CO)_{10}]$	Conv (%)	M_n^{NMR}	PDI	M_n^{GPC}	*R*-CH_2-CF_2	Halide Chain-end	f_{Total}(%)
1	Br-CF_2-$(CF_2)_2$-CF_2-Br[a)]	20/1/0.4	84	4,422	2.69	2,700	***b***, (Q, δ =3.21 ppm)	$\boldsymbol{c}_{Br}$	55
2	Br-CF_2-CH_2-CF_2-Br[a)]	50/1/0.15	25	N/A	1.32	1,000	N/A	$\boldsymbol{c}_{Br}$	76
3	EtOOC-CF_2-Br[b)]	30/1/0.25	24	2,364	1.94	3,400	***b'***, (q, δ = 4.36 ppm and t, δ = 1.33 ppm)	$\boldsymbol{c}_{Br}$	50
4	CF_3-$(CF_2)_2$-CO-Cl[b)]	50/1/0.2	11	N/A	2.03	7,400	N/A	N/A	N/A
5	Cl-CF_2-$(CF_2)_6$-CF_2-Cl[a)]	10/1/0.4	30	5,058	2.16	3,900	***b***, (m, δ = 3.28 ppm)	N/A	N/A
6	Cl-$(CF_2$-$CFCl)_{3\text{-}6}$-Cl[a)]	25/1/0.5	25	5,610	1.71	5,700	***b***, (m, δ = 3.25 ppm; m, δ = 3.4 ppm)	N/A	N/A
7	Cl-CFCl-CF_2-Cl[a)]	50/1/0.15	17	4,735	2.15	5,400	***b***, (m, δ = 3.25 ppm; m, δ = 3.4 ppm)	N/A	N/A
8	$CHCl_3$[a)]	50/1/0.15	10	6,440	2.11	4,600	***b'***, (t, δ = 6.37 ppm)	N/A	N/A
9	Cl_3C-CCl_3[a)]	10/1/0.1	59	N/A	2.00	2,500	***b***, (t, δ = 3.59 ppm)	$\boldsymbol{c}_{Cl}$, $\boldsymbol{c}_{Cl}$'	N/A
10	Cl_3C-Br[a)]	25/1/0.5	22	3,211	1.96	2,400	***b***, (t, δ = 3.75 ppm)	$\boldsymbol{c}_{Br}$, $\boldsymbol{c}_{Br}$', $\boldsymbol{c}_{Cl}$ and $\boldsymbol{c}_{Cl}$'	91
11	CCl_4[a)]	30/1/1	62	4,158	2.19	3,600	***b***, (t, δ = 3.75 ppm)	$\boldsymbol{c}_{Cl}$ and $\boldsymbol{c}_{Cl}$'	N/A
12	CF_3SO_2Cl[a)]	20/1/0.1	10	783	1.85	600	***b***, (tq, δ = 3.24 ppm)	$\boldsymbol{c}_{Cl}$	95

Polymerization was carried out in [a)] ACN, [b)] DMC.

Table S3b. Characterization of PVDF samples initiated from I substrates.

Expt #	Initiator	[VDF]/[I]/ $[Mn_2(CO)_{10}]$	Conv (%)	M_n^{NMR}	PDI	M_n^{GPC}	R-CH_2-CF_2	Halide Chain-end	f_{Total}(%)
1	CH_3-I[a)]	50/1/0.5	20	8,913	1.94	13,900	***b′***, (t, δ =1.02 ppm)	N/A	N/A
2	CH_3-$(CH_2)_4$-CH_2-I[a)]	10/1/0.4	8	696	1.46	3,100	***b′***,(t, δ = 0.88 ppm; m, δ = 1.32 ppm and m, δ = 1.49 ppm)	N/A	N/A
3	I-CH_2-$(CH_2)_8$-CH_2-I[a)]	20/1/0.5	15	N/A	1.83	2,700	***b′***, (m, δ = 1.31 ppm; m, δ = 1.50 ppm and m, δ = 1.60 ppm)	N/A	N/A
4	CF_2H-CF_2-CH_2-I[b)]	50/1/0.2	30	N/A	1.53	1,600	***b′,*** (t, δ = 6.3 ppm)	***c′***	N/A
5	$(CF_3)_3C$-I[a)]	50/1/0.4	59	2,288	1.88	2,500	***b***, m, δ = 3.24 ppm	***c*** and ***c′***	70
6	EtOOC-CF_2-I[c)]	25/1/0.2	84	1,115	1.71	1,200	***b′***, (t, δ = 1.33 ppm; q, δ = 4.36 ppm ; ***b,*** (m, δ = 3.10 ppm)	***c*** and ***c′***	51
7	C_6F_5-CF_2-I[a)]	25/1/0.5	37	1,464	1.36	1,800	***b***, (m, δ =3.30 ppm)	***c*** and ***c′***	54
8	$(CF_3)_2CF$-I[a)]	50/1/0.2	26	1,918	1.39	2,100	***b***, (m, δ = 3.23 ppm)	***c*** and ***c′***	73
9	CF_3-I[a)]	50/10/0.15	30	1,262	1.21	1,400	***b***,(tq, δ = 3.24 ppm)	***c*** and ***c′***	95
10	CF_3-CF_2-I[a)]	50/1/0.1	16	1,185	1.27	1,500	***b***,(Q, δ = 3.20 ppm)	***c*** and ***c′***	93
11	CF_3-$(CF_2)_2$-CF_2-I[c)]	50/1/0.1	30	1,479	1.38	1,300	***b***, (m, δ = 3.24 ppm)	***c*** and ***c′***	81
12	Cl-CF_2-$(CF_2)_4$-CF_2-I[a)]	50/1/0.3	58	1,572	1.56	1,400	***b***, (m, δ = 3.23 ppm)	***c*** and ***c′***	78
13	Cl-CF_2-CFCl-I[c)]	50/1/0.1	30	1,385	1.36	1,100	***b***, (m, δ = 3.22 ppm and m, δ = 3.39 ppm)	***c*** and ***c′***	94
14	I-CF_2-$(CF_2)_2$-CF_2-I[c)]	50/1/0.4	34	2,144	1.38	2,000	***b***, (m, δ = 3.16 ppm)	***c*** and ***c′***	95
15	I-CF_2-$(CF_2)_4$-CF_2-I[c)]	50/1/0.4	41	1,921	1.44	1,800	***b***, (m, δ = 3.22 ppm)	***c*** and ***c′***	96

Polymerization was carried out in [a)]ACN, [b)] Acetone, c) DMC.

Table S3c. PVDF structural assignments of ^{1}H and ^{19}F NMR resonances. The chemical shift values correspond to structures in red italics.

Signal	Structure	^{1}H-NMR	^{19}F-NMR
a	-CF_2-[***CH_2-CF_2***]$_n$-CH_2- HT	m, δ = 2.9 ppm	m, δ = -91.3 ppm
a'	-CH_2-CF_2-CH_2-***CF_2-CF_2-CH_2-CH_2***-CF_2-CH_2-CF_2- HH	m, δ = 2.35 ppm	m, δ = -113.5 ppm
a'$_1$	-CH_2-CF_2-CH_2-CF_2-***CF_2***-CH_2-CH_2-CF_2-CH_2-CF_2- HH	< 0.5 %	m, δ = -115.9 ppm
a'$_2$	-CH_2-CF_2-CH_2-CF_2-CF_2-CH_2-CH_2-***CF_2***-CH_2-CF_2- HH		m, δ = - 95.1 ppm < 0.4 %
a'$_3$	-CH_2-CF_2-***CF_2***-CH_2-CH_2-CF_2-I		m, δ = -115.2 ppm
a'$_4$	-CH_2-CF_2-***CF_2***-CH_2-CH_2-CF_2-H		m, δ = -115.8 ppm
b	PVDF-***CF_2***-C***H_2***-CF_2-CF_2-CF_2-CF_2-CF_2-CF_2-C***H_2***-***CF_2***-PVDF	q, δ = 3.22 ppm	m, δ = -91.8 ppm
b	CF_3-CF_2-CF_2-CF_2-***CH_2-CF_2***-PVDF	q, δ = 3.24 ppm	m, δ = -91.8 ppm
b$_1$	PVDF-CF_2-CH_2-***CF_2***-CF_2-CF_2-CF_2-CF_2-***CF_2***-CH_2-CF_2-PVDF	N/A	m, δ = -111.7 ppm
b$_2$	PVDF-CF_2-CH_2-CF_2-***CF_2***-CF_2-CF_2-***CF_2***-CF_2-CH_2-CF_2-PVDF	N/A	m, δ = -121.2 ppm
b$_3$	PVDF-CF_2-CH_2-CF_2-CF_2-C***F_2***-C***F_2***-CF_2-CF_2-CH_2-CF_2-PVDF	N/A	m, δ = -123.1 ppm
b$_4$	***CF_3***-CF_2-CF_2-CF_2-CH_2-CF_2-PVDF	N/A	m, δ = -80.9 ppm
b$_5$	CF_3-***CF_2***-CF_2-CF_2-CH_2-CF_2-PVDF	N/A	m, δ = -125.5 ppm
b$_6$	CF_3-CF_2-***CF_2***-CF_2-CH_2-CF_2-PVDF	N/A	m, δ = -123.9 ppm
b$_7$	CF_3-CF_2-CF_2-***CF_2***-CH_2-CF_2-PVDF	N/A	m, δ = -111.9 ppm
c	-CH_2-CF_2-CH_2-CF_2-***CH_2-CF_2***-I	q, δ = 3.62 ppm	t, δ = -38.5 ppm
c$_1$	-CH_2-CF_2-CH_2-***CF_2-CH_2***-CF_2-I	$f^{H}_{CF2\text{-}I}$ = 70 %	q, δ = -92.5 ppm, $f^{F}_{CF2\text{-}I}$ = 68 %
c$_2$	-CH_2-CF_2-CF_2-CH_2-CH_2-***CF_2***-I		m, δ = -39.3 ppm,
c'	-CH_2-CF_2-***CF_2-CH_2***-I	t, δ = 3.87 ppm	m, δ = -108.3 ppm $f^{F}_{CH2\text{-}I}$ = 24 %
c'$_1$	-CH_2-***CF_2***-CF_2-CH_2-I	$f^{H}_{CH2\text{-}I}$ = 25 %	m, δ = -112.0 ppm,
d	-CH_2-CF_2-CH_2-***CF_2-H***	tt, δ = 6.3 ppm $f^{H}_{CF2\text{-}H}$ = 4%	dt, δ = -114.7 ppm $f^{F}_{CF2\text{-}H}$ = 6%
d$_2$	-CH_2-CF_2-CF_2-CH_2-CH_2-***CF_2***-H		dt, δ = -116.8 ppm
d'	-CH_2-CF_2-***CF_2-CH_3***	t, δ = 1.80 ppm	dd, δ = -108.2 ppm, $f^{F}_{CF2\text{-}CH3}$ = 2%
d'$_1$	-CH_2-***CF_2***-CF_2-CH_3	$f^{H}_{CF2\text{-}CH3}$ = 1%	δ = -114.1 ppm

NMR Discussion

Examples of the d_6-acetone, ^{1}H-NMR PVDF spectra are presented in Figure S2a (R-X, R_F-X, X = Cl, Br) and Figure S2b (R-I and R_F-I) and summarized in Table S3a,b. A comparison of the ^{1}H and ^{19}F-NMR of I-PVDF-I is presented in Figure S2c and Table S3c, while a comparison of the ^{19}F-NMR spectra of PVDF-I and PVDF-H is shown in Figure S2d,e and Table S3c.

1H-NMR

In addition to known PVDF H-NMR resonances,[3-6] acetone is seen at δ = 2.05 ppm and H_20 at δ = 2.84 ppm.[7] The other sets of signals are associated with PVDF propagation and termination events and respectively with the specific initiator used.

PVDF Main Chain Resonances: Two dominant, propagation derived PVDF main chain signals are observed: First, the head to tail (HT), -CF_2-[C***H***$_2$-CF_2]$_n$-CH_2-, broad multiplet ***a***, appears at δ = 2.8 - 3.1 ppm. Second, the head to head (HH) -(CH_2-CF_2)$_n$-CF_2-C***H***$_2$-C***H***$_2$-CF_2-(CH_2-CF_2)$_m$- linkage (typically HH = 5-10 % in free radical VDF polymerizations) [4,5,8,9,10,11] ***a'*** is observed at δ = 2.3 - 2.4 ppm. Conversely, the resonances derived from typical PVDF termination by the recombination[12] of terminal HT or HH units cannot be easily identified due to overlap, as follows: HT/HT (-CH_2-CF_2-C***H***$_2$-CF_2-CF_2-C***H***$_2$-CF_2-CH_2-, overlap with the HT main chain), HT/HH (-CH_2-CF_2-C***H***$_2$-CF_2-C***H***$_2$-CF_2-CF_2-CH_2-, identical to HT propagation), or HH/HH (-CH_2-CF_2-CF_2-C***H***$_2$-C***H***$_2$-CF_2-CF_2-CH_2-, identical to HH propagation). Interestingly, such termination is dramatically suppressed in the presence of active perfluoroiodo CT agents,[3,13-15] and is visualized by the disappearance of the HH peak a'[14] which becomes -CF_2-C***H***$_2$-I (***c'*** *vide infra*).

Initiator Chain Ends: The second set of signals, ***b*** and ***b'*** correspond to the first VDF unit connected with R_F (R_F-C***H***$_2$-CF_2-) and the R_H initiator fragment, and confirm the predominantly regiospecific[15-17] 1,2-connectivity (R_F-C***H***$_2$-CF_2-) and favored for larger size of R or R_F.

Halide Chain Ends: The ***c*** and ***c'*** resonances represent the corresponding PVDF halide chain ends (*i.e.* HT: ***c***, -CH_2-CF_2-C***H***$_2$-CF_2-X and HH: ***c'***, -CH_2-CF_2-CF_2-C***H***$_2$-X), and in essence, quantify the CT ability of the initiator. Since $Mn(CO)_5$-X is not a halide donor[18] the concentration of ***c*** and ***c'*** may decrease with increasing the amount of $Mn_2(CO)_{10}$ employed. Their ratio will also depend on conversion for X = I. The **c**/**c'** ratio is less affected by conversion for Cl and Br initiators which are not capable of DT under polymerization conditions. However, similarly to VAc,[18] it does change in the favor of the less reactive -CH_2-CF_2-CF_2-CH_2-X for pefluoroiodo derivatives (Figure S4).

H Chain Ends: While dramatically suppressed in IDT, termination can may also occur by H transfer to the HT ~CH_2-$CF_2^\bullet$ or to a smaller extent to the HH ~CF_2-$CH_2^\bullet$ propagating units to form -CH_2-CF_2-***H*** (peak ***d***, triplet of triplets at δ = 6.3 ppm $^3J_{HH}$ = 4.6 Hz $^2J_{HF}$ = 54.7 Hz) and respectively, -CH_2-CF_2-***H*** (peak ***d'***, triplet at 1.80 ppm, $^3J_{HF}$ = 19.2 Hz).[4,19] Such H-transfers may arise from either the solvent, the main chain (inter or intramolecular), or by disproportionation with the terminal HT unit, to also give a -CH_2-CF_2-C***H***=CF_2 unsaturation, observed in a few cases as a trace multiplet at **b"** at ~ 5.2 ppm.

Solvent-derived chain ends: Chain transfer to an R_S-H solvent may occur by H abstraction leading to the -CH_2-CF_2-*H* and -CF_2-CH_2-*H* chain ends described above. This will happen especially when the C-X bond of the initiator or the chain end is very strong, *i.e.* for very weak CT agents.

For most typical R_S-H solvents, the resulting $R_S^{\bullet}$ radicals are not reactive enough to reinitiate VDF and are consumed by dimerization. Thus, the solvent fragment will not be observed in NMR. This is the case of ACN (NC-CH_2-H). Indeed, while $Mn_2(CO)_{10}$ clearly activates the corresponding iodide NC-CH_2-I (Table S1, exp 74), no polymer is obtained, as the resulting CN-stabilized radical dimerizes without addition to VDF (*i.e.* chain breaking and transfer without reinitiation) and is thus absent from the NMR of the polymer.

By contrast, a more reactive CH_3-O-CO-O-CH_2-$^{\bullet}$ radical is generated by H abstraction from DMC. Thus, DMC provides chain transfer *with reinitiation*, (*i.e.* without breaking the radical chain) and this can be seen as trace signals for the poor initiators (*e.g.* CF_3-$(CF_2)_2$-CO-Cl) as C***H*****$_3$**-O-CO-O-C***H*****$_2$**-CH_2-CF_2- at δ = 3.74 s, 3H and respectively at δ = 4.33 ppm, t, 2H. However, this transfer is not observed for the linear perfluoroalkyl iodides suitable for VDF-CRP.

Functionality and Mn calculations.

Comparative integrations of the ***a, a' b, c, c'***, ***d*** and ***d'*** resonances allow the calculation of the halide and hydride chain end functionality, as well as that of M_n^{NMR}, as outlined below and reported in Table S3 :

$$M_n^{NMR} = R_F + N\left\{64.04\left[\frac{\int a+\int a'+\int b+\int c+\int c'+{}^2/_3\int d'}{\int b}\right] + 1.008\left(\frac{2\int d+{}^2/_3\int d'}{\int b}\right) + Y\left(\frac{\int c+\int c'}{\int b}\right)\right\} \quad (1)$$

$$\%\ total\ Iodine\ Functionality = \frac{\int c+\int c\prime}{\int b} = \frac{\int c+\int c\prime}{\int c+\int c\prime+{}^2/_3\int d'+2\int d} \quad (2)$$

$$\%\ \mathrm{CH_2\text{-}CF_2\text{-}I}\ Functionality = \frac{\int c}{\int b} = \frac{\int c}{\int c+\int c\prime+{}^2/_3\int d'+2\int d} \quad (3)$$

$$\%\ \mathrm{CF_2\text{-}CH_2\text{-}I}\ Functionality = \frac{\int c\prime}{\int b} = \frac{\int c\prime}{\int c+\int c\prime+{}^2/_3\int d'+2\int d} \quad (4)$$

$$\%\ \mathrm{CF_2\text{-}CH_2\text{-}H}\ Functionality = \frac{{}^2/_3\int d'}{\int b} = \frac{{}^2/_3\int d'}{\int c+\int c\prime+{}^2/_3\int d'+2\int d} \quad (5)$$

$$\%\ \mathrm{CH_2\text{-}CF_2\text{-}H}\ Functionality = \frac{2\int d}{\int b} = \frac{2\int d}{\int c+\int c\prime+{}^2/_3\int d'+2\int d} \quad (6)$$

Where 1.008 and 64.04, represent the molar masses of H and VDF while Y is the atomic wt of the halide chain end (*e.g.* Y = 126.9 for iodine chain ends); N = 1, 2 (initiator functionality); and R_F is the mol. wt of the initiator fragment (without the halides). All integrals are normalized to 2 protons.

The initiation from each halide is described below as follows:

(a) Cl and Br initiators:

CF_3-SO_2-Cl: As for other R_F-SO_2-Cl derivatives, SO_2 extrusion occurs upon radical formation[20-22] and peak ***b***, CF_3-C*H*$_2$-CF_2-CH_2-CF_2-,[15] is seen at δ = 3.24 ppm, (*tq* $^3J_{HF}$ = 10.3 Hz, $^3J_{HF}$ = 5.2 Hz). As described later, this is identical with initiation from CF_3-I and similar with that from most R_F-X initiators. Peak ***c***, δ = 3.44 ppm, [6] (*tt,* $^3J_{HF}$ = 14.6 Hz) corresponds to the HT -CF_2-C*H*$_2$-CF_2-Cl chain end, while, the -CF_2-CF_2-C*H*$_2$-Cl ***c'*** chain end is not observed. The high value of *f* = 0.89 reflects the good CT ability of this initiator which has a very labile SO_2-Cl bond. Remarkably, very little HH content or H transfer are observed.

CCl_4: Since polyhalide radicals add regioselectively onto the CH_2 side of VDF,[16] the CCl_3-CF_2-C*H*$_2$-CF_2-CH_2- minor isomer if any, is probably masked by the main chain. Thus, the dominant CCl_3-C*H*$_2$-CF_2-CH_2-CF_2-, ***b***, is observed at δ = 3.75 ppm[6,23] (*t*, $^3J_{HF}$ = 14.8 Hz) whereas the halide chain end ***c***, -C*H*$_2$-CF_2-Cl is seen at δ = 3.44 ppm[6] (*tt,* $^3J_{HF}$ = 14.4Hz) and even traces of -CF_2-C*H*$_2$-Cl (**c**' = 7% of *d*) can be seen at δ = 4.04 ppm (*t*, $^3J_{HF}$ = 13.6 Hz). A partial overlap of ***c*** with possible difunctional initiation -CF_2-C*H*$_2$-CCl_2-C*H*$_2$-CF_2- is seen at δ = 3.36 ppm (*t*, $^3J_{HF}$ = 16 Hz). The chain end functionality is *f* = 0.47.

CCl_3Br: Similarly to CCl_4, the CCl_3-C*H*$_2$-CF_2-CH_2-CF_2-, ***b***, is again observed at δ = 3.75 ppm[6,23] (*t*, $^3J_{HF}$ = 14.8 Hz) whereas the ***c$_{Br}$***, and ***c$_{Br}$'*** bromine chain ends -C*H*$_2$-CF_2-Br and -CF_2-C*H*$_2$-Br are seen at δ = 3.56 ppm[6,19,24,25] (*tt,* $^3J_{HF}$ = 15.2Hz) and respectively δ = 3.94 ppm (*t*, $^3J_{HF}$ = 14.4 Hz).[6,24] Interestingly, Cl-derived -CH_2-C*F*$_2$-Cl and -CF_2-C*H*$_2$-Cl chain ends (***c$_{Cl}$*** and ***c'$_{Cl}$*** can also be seen at δ = 4.04 ppm (*t*, $^3J_{HF}$ = 13.6 Hz) and respectively δ = 3.45 ppm (*q*, $^3J_{HF}$ = 14.6 Hz). While the less active -CF_2-C*H*$_2$-Cl appears to be of a similar intensity with -C*H*$_2$-CF_2-Br, this is simply because the excess $Mn_2(CO)_{10}$ used in this reaction has already irreversibly abstracted Br from the more reactive -C*H*$_2$-CF_2-Br chain end, thus decreasing its concentration. Moreover, trace difunctional initiation can be distinguished (-CF_2-C*H*$_2$-CCl_2-C*H*$_2$-CF_2, (δ = 3.37 ppm, *q*, $^3J_{HF}$ = 15.6 Hz). As CCl_3Br is a much better VDF CT agent than CCl_4,[16] a better chain end functionality is expected.

CCl_3-CCl_3: The connectivity peak ***b*** CCl_3-CCl_2-C*H*$_2$-CF_2- appears at δ = 3.59 (t, $^3J_{HF}$ = 15 Hz). The ***c*** -C*H*$_2$-CF_2-Cl and ***c***' -CF_2-C*H*$_2$-Cl halide chain ends can be seen at δ = 3.45 ppm, ($^3J_{HF}$ = 14.6 Hz) and respectively δ = 4.04 ppm (*t*, $^3J_{HF}$ = 13.6 Hz). Trace difunctional initiation seen as -CF_2-C*H*$_2$-CCl_2-CCl_2-C*H*$_2$-CF_2-, δ = 3.49 ppm ($^3J_{HF}$ = 16.2 Hz) whereas the multiplets at 3.1-3.3 ppm most likely correspond to a combination of CCl_3-CCl_2-CH_2-CF_2-C*H*$_2$-CF_2- at δ = 3.15 ppm and the 2,1-reverse addition CCl_3-CCl_2-CF_2-C*H*$_2$-CF_2- at 3.25 ppm (*quintet*, $^3J_{HF}$ = 16.1 Hz).

$CHCl_3$: The initiator connectivity can be observed *via* the ***b'*** resonances of the *H*-CCl_2-CH_2-CF_2- (*t*, δ = 6.37 ppm, $^3J_{HH}$ = 6.1 Hz) 1,2-addition fragment, partially overlapping with the CH_2-CF_2-H chain end (***d***), and *via* the trace *H*-CCl_2-CF_2-CH_2 (multiplets at δ = 6.45 ppm - 6.53 ppm) corresponding to the less frequent 2,1-addition. Since neither CH_2Cl_2 nor Cl-CHCl-CHCl-Cl did initiate polymerization, it is unlikely that $CHCl_3$ is capable of a second initiation. The first VDF unit ***b*** $HCCl_2$-C*H*$_2$-CF_2- is seen at δ = 3.13 ppm (*td* $^3J_{HH}$ = 6.2 Hz, $^3J_{HF}$ = 9.8 Hz) while the $HCCl_2$-CF_2-C*H*$_2$- unit is not observed. However, no ***c*** or ***c'*** halide chain ends were detected since $CHCl_3$ is a much poorer VDF CT agent[16] than CF_3-SO_2Cl, CCl_4 and CCl_3Br.

Cl-CFCl-CF_2-Cl (Freon): In this case, mono and difunctional initiation is possible and thus the first VDF units ***b***, *i.e.* Cl-CF_2-CFCl-C*H*$_2$-CF_2- and Cl-CFCl-CF_2-C*H*$_2$-CF_2- are seen as multiples at δ = 3.4 ppm and respectively δ = 3.25 ppm. Conversely, the 2,1-addition from the more reactive

(*Cl*-CFCl-CF_2-Cl) side would afford Cl-CF_2-CFCl-CF_2-C*H*$_2$-CF_2- with a very similar chemical shift. Again, the ***c*** and ***c'*** -C*H*$_2$-CF_2-Cl and -CF_2-C*H*$_2$-Cl halide chain ends are absent, indicating that similarly to $CHCl_3$, Cl-CFCl-CF_2-Cl is a very poor VDF CT agent.

Halocarbon oil: Cl-(CF_2-CFCl)$_{3\text{-}6}$-Cl. This oligomeric multifunctional initiator closely resembles Cl-CFCl-CF_2-Cl (Freon) and perfluoro isopropyl chloride CF_3-CFCl-CF_3. Thus, like Freon, the initiator connectivity peak (~CH_2-CF_2)$_2$CF-C*H*$_2$-CF_2- appears as a multiplet at δ = 3.4 ppm whereas initiation from the -CF_2-Cl termini of halocarbon oil appears at δ = 3.25 ppm. While the secondary C-Cl bond here may be weaker than -CF_2-Cl, $Mn_2(CO)_{10}$ preferentially activates primary halides.[26] Similarly to all perfluoro chlorides, no -CF_2-C*H*$_2$-Cl or -CH_2-CF_2-Cl chain ends are seen due to the very poor CT ability of this initiator. However, this initiator represents a model of for the future synthesis of PVDF stars or grafting of PVDF from polymer halides.

Cl-CF_2-(CF_2)$_6$-CF_2-Cl: The initiation is demonstrated by the ***b*** multiplet at δ = 3.28 ppm assigned to -CF_2-C*H*$_2$-(CF_2)$_8$-C*H*$_2$-CF_2-. Similarly to all perfluoro chlorides, no -CF_2-C*H*$_2$-Cl or -C*H*$_2$-CF_2-Cl halide chain ends can be seen.

CF_3-(CF_2)$_2$-CO-Cl: The CF_3-(CF_2)$_2$-CO-C*H*$_2$-CF_2- is most likely overlapping with the PVDF main chain and again no halide chain end is observed.

EtOOC-CF_2-Br: The ***b'*** initiator peaks (C*H*$_3$-CH_2-O- and CH_3-C*H*$_2$-O- are seen at δ = 1.33 ppm (*t*, $^3J_{HH}$ = 7.15 Hz) and respectively at δ = 4.36 ppm (*q*, $^3J_{HH}$ = 7.09 Hz) whereas the initiator connectivity is revealed by the EtOOC-CF_2-C*H*$_2$-CF_2- resonance ***b*** δ = 3.11 ppm, $^3J_{HF}$ = 15.57 Hz. The -CF_2-C*H*$_2$-CF_2-Br is observed at δ = 3.55 ppm (*q*, $^3J_{HF}$ = 15 Hz).[6,19,24,25] and the -CF_2-C*H*$_2$-Br resonance is absent. A reasonable chain end functionality *f* = 0.5 is available for this initiator.

Br-CF_2-CH_2-CF_2-Br: The initiator connectivity with PVDF is undetectable as it provides the same structure as the HT main chain. However, the ***c*** -CF_2-C*H*$_2$-CF_2-Br halide chain end is observed at δ = 3.55 ppm (*q*, $^3J_{HF}$ = 15 Hz)[6,19,24-25] while the **c'** -CF_2-C*H*$_2$-Br resonance is absent, indicating that no DT is in effect (otherwise it would accumulate). This initiator also represents a model of the higher reactivity 1,2-halide chain end unit.

Br-CF_2-CF_2-CF_2-CF_2-Br: The first VDF unit -(CF_2)$_4$-C*H*$_2$-CF_2- is seen at δ = 3.21 ppm (*q*, $^3J_{HF}$ = 15 Hz). The -CF_2-C*H*$_2$-CF_2-Br halide end is observed at δ = 3.55 ppm (*q*, $^3J_{HF}$ = 15 Hz).[6,19,24-25] and again the -CF_2-C*H*$_2$-Br resonance is not observed, indicating that no Br-DT is in effect.

(b) Iodo Initiators:

Alkyl Iodides:

CH_3-I: The initiator derived chain ends[4,27] of the dominant 1,2-addition are seen as C*H*$_3$-CH_2-CF_2- (δ = 1.02 ppm, $^3J_{HH}$ = 7.5Hz) and CH_3-C*H*$_2$-CF_2- (m, δ = 2 ppm, under the acetone peak). The less favored 2,1-addition, C*H*$_3$-CF_2-CH_2-CH_2-CF_2- (t, δ = 1.55 ppm), or the termination *via* H abstraction onto a HH unit C*H*$_3$-CF_2-CF_2-CH_2-CF_2- (tt, δ = 1.80) are not observed. Moreover, no iodine chain ends are detected, indicating that CH_3-I is a very poor CT agent.

CH_3-(CH_2)$_4$-CH_2-I: The initiation is demonstrated by the alkyl resonances with C*H*$_3$-(CH_2)$_5$-, δ = 0.88 ppm (*t*, 3H, $^3J_{HH}$ = 7 Hz), CH_3-(C*H*$_2$)$_4$-CH_2-CH_2-CF_2- δ = 1.32 (broad multiplet 1.24-1.41 ppm, 6.8 H), and CH_3-(CH_2)$_4$-C*H*$_2$-CH_2-CF_2-, δ = 1.49 ppm (m, 1.2 H). The integral mismatch indicate ~ 15 % 2,1-addition, where the last methylene of the initiator (CH_3-(CH_2)$_4$-C*H*$_2$-CF_2-CH_2-CH_2-CF_2-) and the methylene of the first VDF 1,2-unit (CH_3-(CH_2)$_4$-CH_2-C*H*$_2$-CF_2-) overlap with acetone. Again, no iodo chain ends are observed.

I-CH_2-$(CH_2)_8$-CH_2-I: The initiator alkyl peaks are all observed as multiplets as follows: PVDF-CH_2-CH_2-CH_2-(C*H*$_2$)$_4$-CH_2-CH_2-CH_2-PVDF-, δ = 1.31 ppm, PVDF-CH_2-CH_2-C*H*$_2$-$(CH_2)_4$-C*H*$_2$-CH_2-CH_2-VDF-, δ = 1.50 ppm, VDF_n-CH_2-C*H*$_2$-CH_2-$(CH_2)_4$-CH_2-C*H*$_2$-CH_2-VDF_n-, δ = 1.60 ppm, and finally PVDF-C*H*$_2$-CH_2-CH_2-(C*H*$_2$)$_4$-CH_2-CH_2-C*H*$_2$-PVDF-, δ = 1.8 ppm and 2 ppm, depending on the 1,2- and 2,1-addition, and overlapping with terminal CH_3-CF_2- and respectively with acetone. A small C*H*$_3$-CH_2-$(CH_2)_8$-, derived from H chain transfer to the initiator is also seen (t, δ = 0.88 ppm). Once more, no iodo chain ends are present.

Semi and Perfluorinated Iodides.

HCF_2-CF_2-CH_2-I. The initiator resonance, ***b'***, *H*-CF_2-CF_2-CH_2-PVDF seen at δ = 6.3 ppm overlaps with the resonance ***d***, (PVDF-CH_2-CF_2-*H*) corresponding to the termination by H abstraction. Thus, while this triplet may suggest higher termination, it is in fact an initiator fragment.[28] Conversely, the methylene initiator resonance H-CF_2-CF_2-C*H*$_2$-CH_2-CF_2-PVDF, overlaps with the HH PVDF *a*' unit at δ = 2.35 ppm. H-CF_2-CF_2-CH_2-I is the least active iodine initiator in the series for which an iodine chain ends are detected. Thus, resonance ***c'*** *i.e.* -CF_2-C*H*$_2$-I is observed at δ = 3.87 ppm (t, $^3J_{HF}$ = 18.2 Hz). As HCF_2-CF_2-CH_2-I represents a model for the less reactive PVDF-CF_2-CH_2-I chain end, polymer formation here, in conjunction with chain end activation experiments (Figure 2, main text) demonstrate that $Mn(CO)_5^\bullet$ activates not only -CH_2-CF_2-I, but also the less reactive -CF_2-CH_2-I PVDF termini, thus supporting complete chain end activation for block copolymerization.

$(CF_3)_3$C-I. The $(CF_3)_3$C-C*H*$_2$-CF_2- is observed at $\delta = 3.24$ (t, $^3J_{HF}$ = 17.1 Hz) while the less reactive ***c'*** *i.e.* -CF_2-C*H*$_2$-I is observed at δ = 3.88 ppm. This is also the first iodide initiator where the more reactive -C*H*$_2$-CF_2-I chain end is beginning to emerge (***c***, δ = 3.62 ppm, *q*, $^3J_{HF}$ = 16 Hz) The results with this initiator are consistent with the unfavorable attack of $Mn(CO)_5^\bullet$ on tertiary halides as well as with the unflavored attack of very electrophilic radicals onto electrophilic alkenes.

EtOOC-CF_2-I. Similarly to its Br counterpart above, the ***b'*** resonances (C*H*$_3$-CH_2-O- and are CH_3-C*H*$_2$-O- are seen at δ = 1.33 ppm (*t*, $^3J_{HH}$ = 7.15 Hz) and respectively δ = 4.36 ppm (*q*, $^3J_{HH}$ = 7.09 Hz) whereas the initiator connectivity ***b*** resonance EtOOC-CF_2-C*H*$_2$-CF_2- is observed at δ = 3.10 ppm, (m, $^3J_{HF}$ = 15.6 Hz). Both ***c*** and ***c'*** resonances are again present.

C_6F_5-CF_2-I: The PVDF first unit ***b*** C_6F_5-CF_2-C*H*$_2$-CF_2 is seen as a multiplet at δ = 3.30 ppm and the resonances ***c*** and ***c'*** -C*H*$_2$-CF_2-I and -CF_2-C*H*$_2$-I are observed at δ = 3.62 ppm (*q*, $^3J_{HF}$ = 16 Hz) and respectively δ = 3.87 ppm (t, $^3J_{HF}$ = 18.2 Hz) as above.

$(CF_3)_2$CF-I: The first VDF unit $(CF_3)_2$CF-C*H*$_2$-CF_2- ***b***, is seen at δ = 3.23 ppm (*quartet*, $^3J_{HF}$ = 17.5 Hz) with the resonances ***c*** and ***c'*** as above.

CF_3-I: The typically regiospecific CF_3-C*H*$_2$-CF_2 addition[15,29] is evidenced at δ = 3.24 ppm, (*tq,* $^3J_{HF}$ = 10.3 Hz, $^3J_{HF}$ = 5.2 Hz), as already observed for CF_3-SO_2-Cl. In addition, both -CF_2-C*H*$_2$-I and -C*H*$_2$-CF_2-I iodine chain ends units ***c*** and ***c'*** are clearly seen as before.

CF_3-CF_2-I: The first VDF unit ***b*** CF_3-CF_2-C*H*$_2$-CF_2-PVDF is seen at δ = 3.20 ppm, (*quintet,* $^3J_{HF}$ = 17.1 Hz) while both iodine chain ends ***c*** and ***c'*** are again observed as above.

CF_3-$(CF_2)_2$-CF_2-I (PFBI): The first VDF unit ***b***, CF_3-$(CF_2)_4$-CF_2-C*H*$_2$-CF_2 is present at δ = 3.24 ppm, (quintet $^3J_{HF}$ = 17.1 Hz) as are both ***c*** and ***c'*** iodo resonances as above.

Cl-CF_2-$(CF_2)_4$-CF_2-I: Similarly, the ***b*** connectivity is seen at δ = 3.23 ppm, and so are the iodo ***c*** and ***c'*** iodo resonances. However, the Cl chain ends are absent, indicating that no CT is available towards ~CF_2-Cl.

Cl-CF_2-CFCl-I. This initiator bears a strong resemblance with Cl-CF_2-CFCl-Cl and thus, the connectivity peaks (***b***) -CFCl-CF_2-CH_2-CF_2- and ~CF_2-CFCl-CH_2-CF_2- are also observed as multiplets at δ = 3.22 ppm and respectively δ = 3.39 ppm. Interestingly, although the Cl-CF_2- bond is likely stronger than the -FClC-I, this initiator still provides difunctional growth. However, only the I-derived chain ends are present while, as for Freon, the Cl chain ends are not detected.

I-$(CF_2)_4$-I and I-$(CF_2)_6$-I. These structures are difunctional initiators with equal reactivity end groups. The connectivity is demonstrated by the -CF_2-CH_2-$(CF_2)_4$-CH_2-CF_2- and -CF_2-CH_2-$(CF_2)_6$-CH_2-CF_2- ***b*** at δ = 3.16 ppm, (quintet, $^3J_{HF}$ = 16.5 Hz) and respectively at δ = 3.22 ppm, (quintet, $^3J_{HF}$ = 17.1 Hz). In both cases, excellent iodine chain ends are seen in conjunction with greatly diminished termination and HH addition similarly to all good perfluoro iodine initiators.

^{19}F-NMR Characterization of I-PVDF-I, PVDF-I and PVDF-H

A comparison of ^{1}H- and ^{19}F-NMR proton decoupled spectra of I-PVDF-I initiated from I-$(CF_2)_6$-I is provided in Figure S2c, while a comparison of the ^{19}F-NMR spectra of PVDF-I initiated from CF_3-CF_2-CF_2-CF_2-I with the corresponding PVDF-H (obtained by reacting PVDF-I with excess $Mn_2(CO)_{10}$ and corresponding to the top of Figure 2 in the manuscript in the block copolymerization discussion) is shown in Figure S2d,e. The corresponding assignments are presented in Table S3c, using the same notation as for the ^{1}H-NMR spectra. In all cases, the ^{1}H and ^{19}F spectra are in accordance, and give very similar values for functionality or M_n^{MNR}. The ^{19}F assignments are discussed below.

The main chain PVDF HT -CF_2-[***CH_2-CF_2***]$_n$-CH_2- unit ***a*** is observed at δ = -91.3 ppm. While the HH units are greatly minimized in VDF-IDT, *trace* internal HH are seen as a series of 3 resonances -CH_2-CF_2-CH_2-***CF_2***-CF_2-CH_2-CH_2-CF_2-CH_2-CF_2-, -CH_2-CF_2-CH_2-CF_2-***CF_2***-CH_2-CH_2-CF_2-CH_2-CF_2- and -CH_2-CF_2-CH_2-CF_2-CF_2-CH_2-CH_2-***CF_2***-CH_2-CF_2-, peaks ***a'***, ***a'$_1$*** and ***a'$_2$*** at δ = -113.5 ppm, δ = -115.9 ppm and respectively, δ = - 95.1 ppm. Interestingly, *penultimate* -CH_2-CF_2-***CF_2***-CH_2-CH_2-CF_2-I and respectively -CH_2-CF_2-***CF_2***-CH_2-CH_2-CF_2-H HH units can also be distinguished as ***a'$_3$*** and ***a'$_4$*** at δ = -115.2 ppm and δ = -115.8 ppm.

The connectivity of the R_F initiators with the main chain is demonstrated by the resonance ***b***, PVDF-***CF_2***-CH_2-CF_2-CF_2-CF_2-CF_2-CF_2-CF_2-CH_2-***CF_2***-PVDF and respectively CF_3-CF_2-CF_2-CF_2-CH_2-***CF_2***-PVDF associated with the first VDF unit.

The R_F initiator resonances are clearly distinguished as PVDF-CF_2-CH_2-***CF_2***-CF_2-CF_2-CF_2-CF_2-***CF_2***-CH_2-CF_2-PVDF, PVDF-CF_2-CH_2-CF_2-***CF_2***-CF_2-CF_2-***CF_2***-CF_2-CH_2-CF_2-PVDF and PVDF-CF_2-CH_2-CF_2-CF_2-C***F$_2$***-C***F$_2$***-CF_2-CF_2-CH_2-CF_2-PVDF peaks ***b$_1$***, ***b$_2$*** and ***b$_3$*** at δ = -111.7 ppm, δ = -121.2 ppm and δ = -123.1 ppm for I-PVDF-I and respectively as ***CF_3***-CF_2-CF_2-CF_2-CH_2-CF_2-PVDF, CF_3-***CF_2***-CF_2-CF_2-CH_2-CF_2-PVDF, CF_3-CF_2-***CF_2***-CF_2-CH_2-CF_2-PVDF and CF_3-CF_2-CF_2-***CF_2***-CH_2-CF_2-PVDF peaks ***b$_4$***, ***b$_5$***, ***b$_6$*** and ***b$_7$*** at δ = -80.9 ppm δ = -125.5 ppm, δ = -123.9 ppm and δ = -111.9 ppm for PVDF-I and PVDF-H.

The more reactive 1,2-type iodide chain ends are seen as -CH_2-CF_2-CH_2-CF_2-CH_2-***CF_2***-I and -CH_2-CF_2-CH_2-***CF_2***-CH_2-CF_2-I, peaks ***c*** and ***c_1*** at δ = -38.5 ppm and respectively δ = -92.5 ppm, as well as a weaker, penultimate -CH_2-CF_2-CF_2-CH_2-CH_2-***CF_2***-I HH unit, ***c_2*** at δ = -39.3 ppm. The less reactive 2,1-type iodide chain ends are observed as -CH_2-CF_2-***CF_2***-CH_2-I and -CH_2-***CF_2***-CF_2-CH_2-I peaks ***c'*** and ***c'_1*** at δ = -108.3 ppm and respectively δ = -112.0 ppm.

Finally, the complete activation of both iodine chain ends by manganese and their replacement with H, enables the clear confirmation of all "***c***" peaks associated with iodine, *via* their disappearance, as well as that of the -CH_2-CF_2-CH_2-***CF_2***-H, -CH_2-CF_2-CF_2-CH_2-CH_2-***CF_2***-H, -CH_2-CF_2-***CF_2***-CH_3 and -CH_2-***CF_2***-CF_2-CH_3 H chain ends, peaks ***d, d_2, d'*** and ***d'_1*** at δ = -114.7 ppm, δ = -116.8 ppm, δ = -108.2 ppm and respectively δ = -114.1 ppm *via* their comparative increase in intensity in PVDF-H.

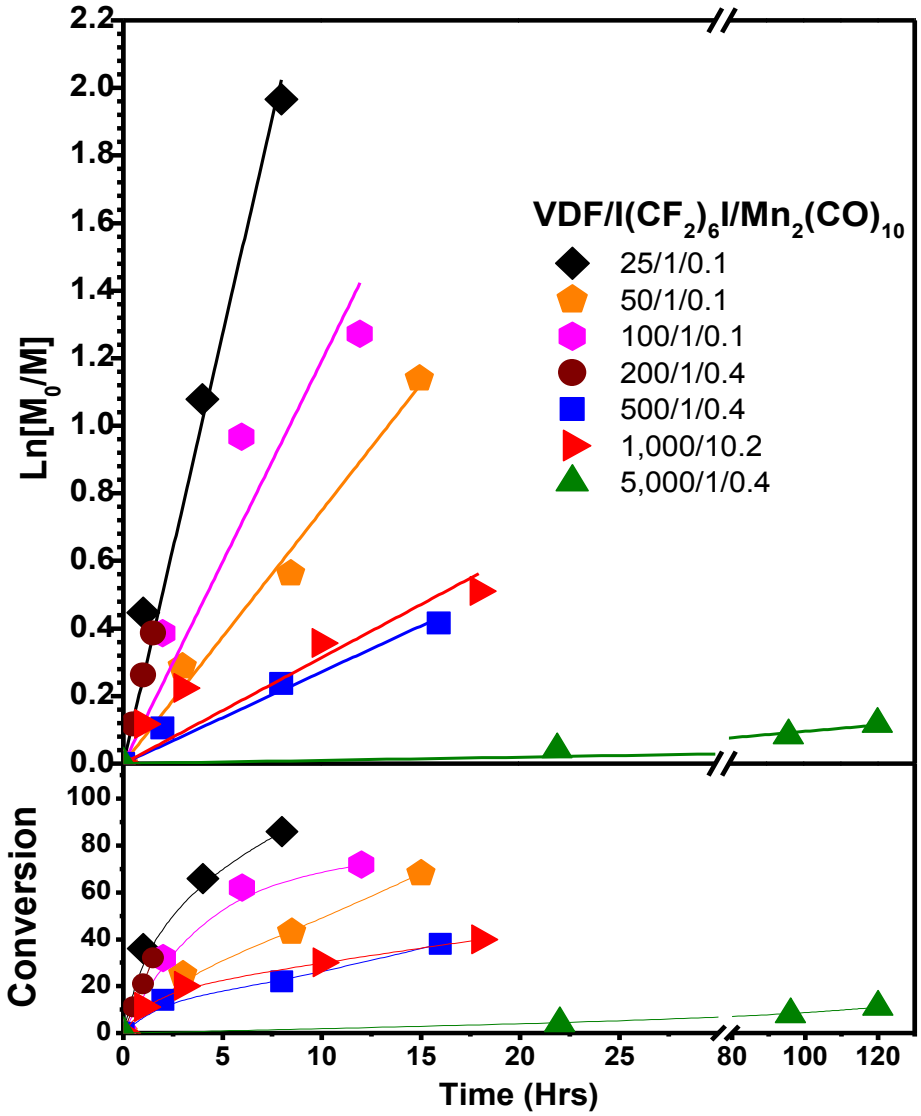

Figure S3. Kinetics of the $Mn_2(CO)_{10}$ photomediated VDF polymerizations at various VDF/I ratios corresponding to Figure 1 in the main text and experiments 43-49 in Table S1.

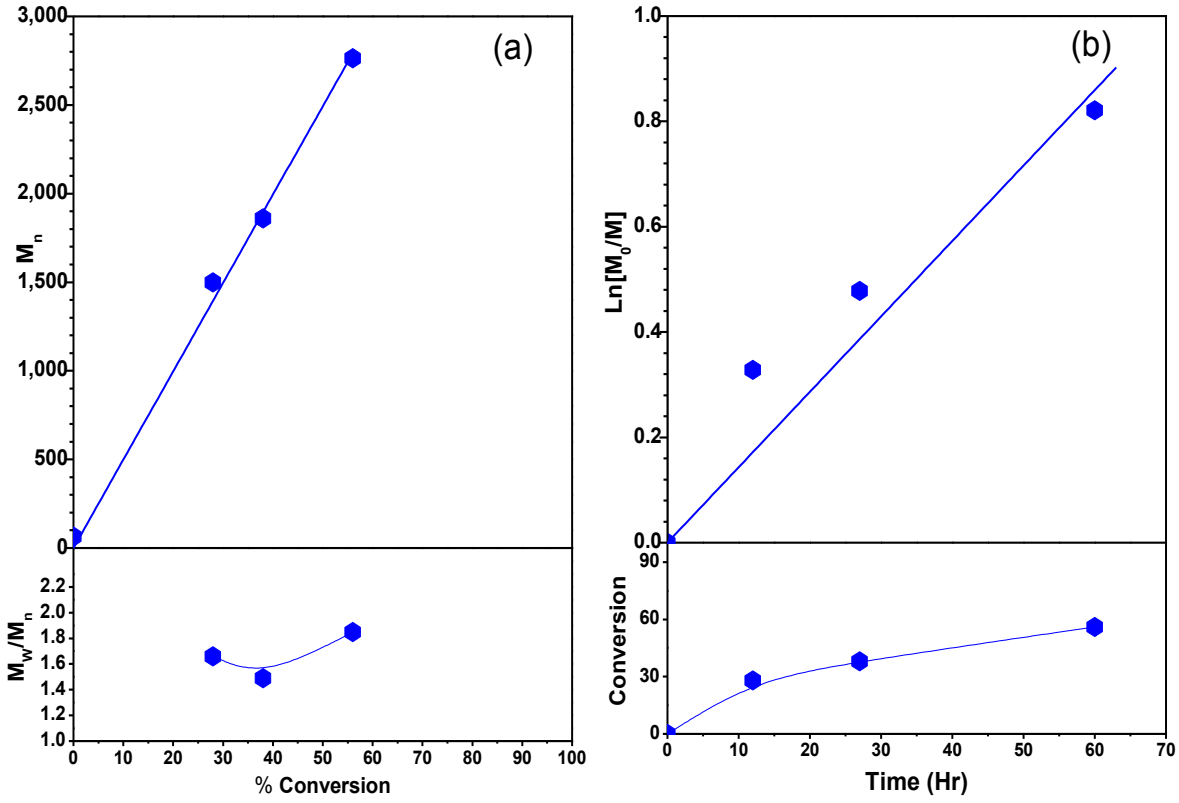

Figure S4. $Mn_2(CO)_{10}$ photomediated synthesis of poly(VDF-*co*-HFP). (a) Dependence of M_n and M_w/M_n on conversion; (b) First order kinetics. [VDF]/[HFP]/[CF_3-CF_2-CF_2-CF_2-I]/[$Mn_2(CO)_{10}$] = 80/20/1/0.2, T = 40 °C

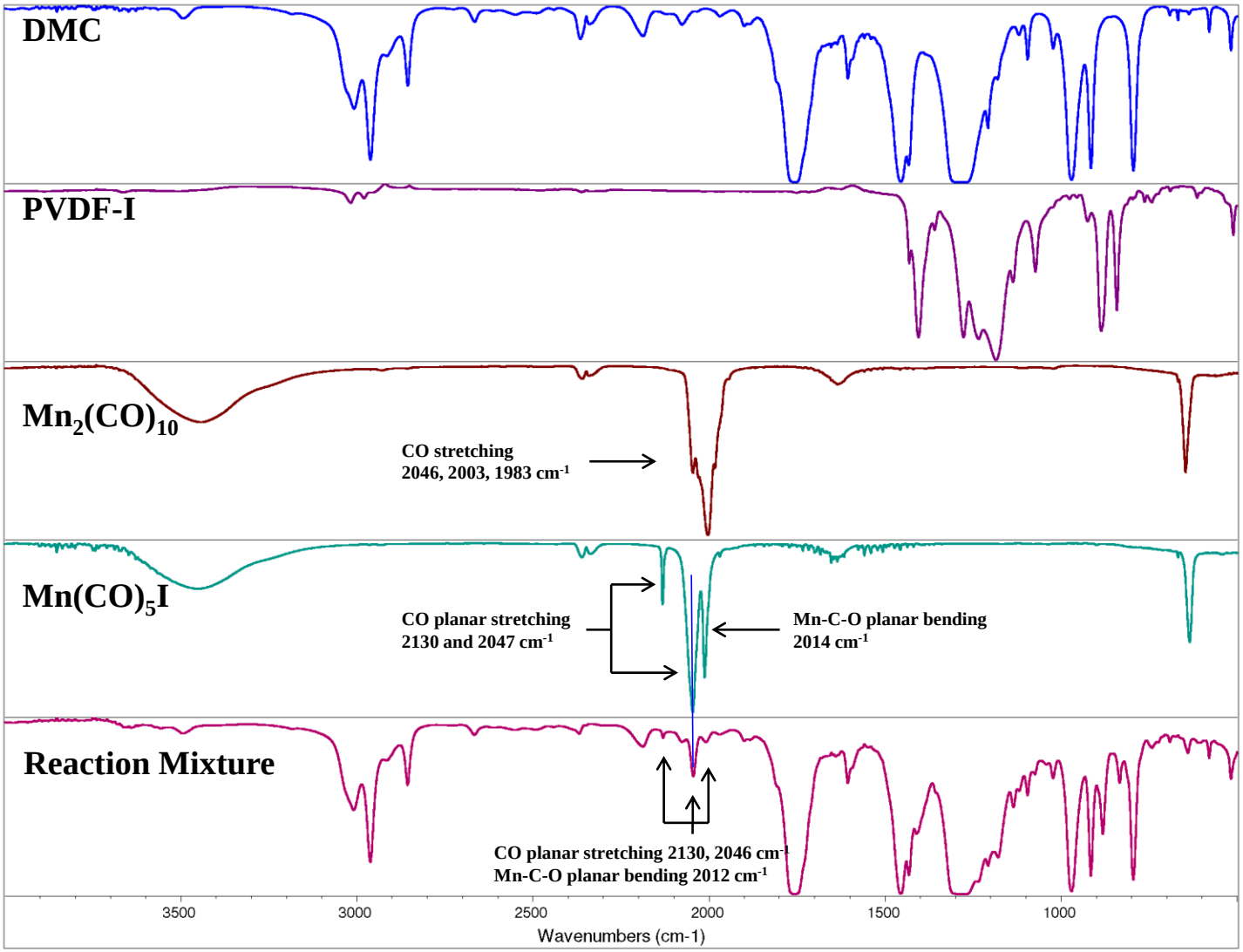

Figure S5a. Comparison of IR spectra of DMC, PVDF-I, $Mn_2(CO)_{10}$, $Mn(CO)_5$-I and of a typical polymerization mixture ([VDF]/[PFBI]/[$Mn_2(CO)_{10}$] = 25/1/0.2, after evaporation of VDF, ~ 80 % conversion).

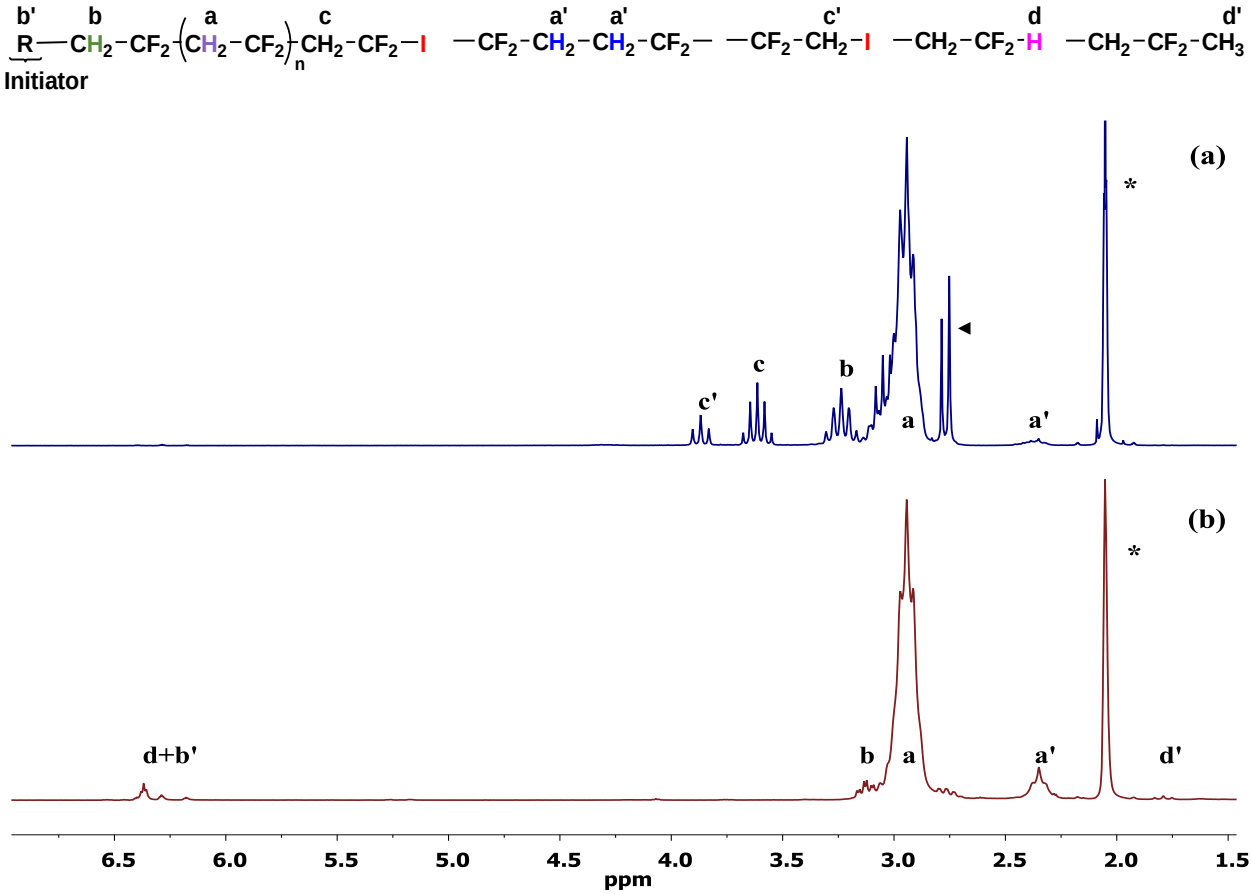

Figure S5b. Effect of excess $Mn(CO)_5$-I: Comparison of the 500 MHz ^{1}H-NMR d_6-acetone spectra of (a) PVDF-I obtained from VDF/PFBI/$Mn_2(CO)_{10}$ = 50/1/0.1 with (b) PVDF obtained from VDF/$CHCl_3$/$Mn_2(CO)_{10}$/$Mn(CO)_5$-I = 50/1/0.2/1, ◀ = H_2O, * = acetone.

Figure S5 Discussion.

Figure S5 addresses the issue of whether or not $Mn_2(CO)_5$-I can donate I back to the propagating chain. In fact, this is not possible under the reaction conditions, since the BDE of $Mn_2(CO)_5$-I (54 kcal/mol)[30] is larger than that of typical R_F-I (*e.g.* for $CF_3CF_2CF_2CF_2$-I, BDE = 48.4 kcal/mol).[31] In addition, R-I compounds are most likely already in a photoexcited state, activated towards homolysis,[32] prior to their interaction $Mn_2(CO)_5^{\bullet}$. By contrast, the Mn-I bond of $Mn(CO)_5$-I does not photolyze homolytically under visible irradiation.[33]

Thus, in Figure S5a the characteristic IR frequencies of $Mn_2(CO)_5$-I (2130, 2046, 2012 cm-^{1})[2,34] are clearly observed in both the $Mn_2(CO)_5$-I pure sample and in the reaction mixture.

Conversely, Figure S5b compares a typical PVDF-I sample with PVDF synthesized from $CHCl_3$, (an initiator which is a very poor chain transfer agent and cannot generate any PVDF-Cl chain ends) in the presence of a large excess of $Mn_2(CO)_5$-I. Thus, if any iodine abstraction by the propagating chain from $Mn_2(CO)_5$-I would be possible, the corresponding PVDF-I chain ends PVDF-C*H*$_2$-CF_2-I and PVDF-CF_2-C*H*$_2$-I (**c** and **c'** δ = 3.62 ppm δ = 3.87 ppm) would be visible. This is clearly not the case.

Together, these control experiments indicate that similarly to the IDT of vinyl acetate,[35] (ref 22 in the manuscript) the reversible iodine transfer is not mediated by $Mn_2(CO)_5$-I.

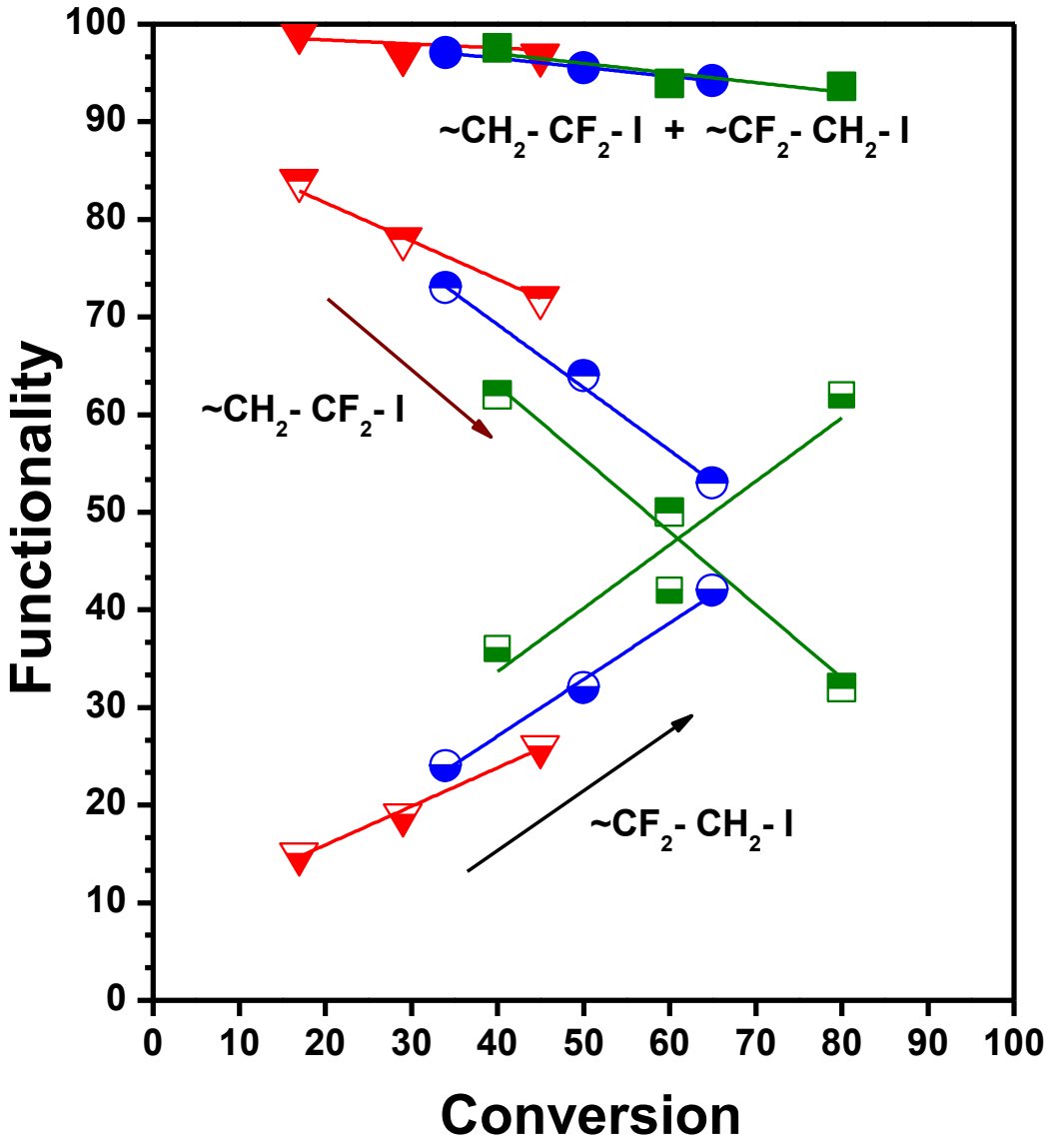

Figure S6. Dependence of halide chain end functionality on conversion in the $Mn_2(CO)_{10}$ mediated CRP of VDF, rt, visible light. [VDF]/[$I(CF_2)_6I$]/[$Mn_2(CO)_{10}$] = 50/1/0.1 (▼), 50/1/0.2 (●), 50/1/0.4 (■). Filled symbols = total functionality, top filled = ~CH_2-CF_2-I, bottom filled = ~CF_2-CH_2-I.

The functionality was determined by NMR, from the integration of the initiator derived chain ends -CF_2-CH_2-$(CF_2)_6$-CH_2-CF_2- at δ = 3.22 ppm vs. the corresponding **c** and **c**' *i.e.* -CH_2-CF_2-I and -CF_2-CH_2-I iodide chain ends observed at δ = 3.62 ppm and respectively δ = 3.87 ppm.

Table S4. Characterization of $Mn_2(CO)_{10}$ Photomediated Synthesis of PVDF Block Copolymers and PVDF chain extensions.

Exp.	Monomer M	PVDFI or I-PVDF-I M_n	PDI	[M]/[PVDFI]/ [$Mn_2(CO)_{10}$]	Conv (%)	Composition M/VDF	M_n	PDI
1	Styrene[a,b)]	2,500	1.34	60/1/2	67	70/30	14,500	2.25
2	Styrene[a,b)]	11,500	1.48	4,000/1/5	12	92/8	44,700	1.92
3	Butadiene[b)]	1,400	1.48	200/1/1	25	62/38	4,700	2.00
4	Vinyl Chloride[c)]	1,800	1.29	100/1/1	35	77/23	20,100	1.52
5	Vinyl Acetate	1,500	1.49	100/1/0.2	30	65/35	11,000	1.70
6	Methyl Acrylate	2,300	1.52	75/1/4	40	72/28	9,000	2.46
7	Acrylonitrile[a)]	2,100	1.31	50/1/1	25	74/26	25,800	2.33
8	VDF [a,d)]	8,000	1.45	750/1/0.1	20	0/100	19,500	1.63
9	VDF [a,d)]	17,000	1.34	2,500/1/0.3	7	0/100	31,300	1.69

Block copolymers from PVDF-I at T = 40 °C and solvent = DMAC except where noted: [a)]Block copolymers from I-PVDF-I samples. [b)] T = 110 °C, [c)]In dioxane, [d)]In DMC.

The NMR assignments corresponding to the copolymers from Figure 2 are as follows:
Polystyrene:
e, δ = 6.4-7.4 ppm, -CH_2-CH(C_6H_5)-,
e' δ = 1.94 ppm , -CH_2-C*H*(C_6H_5)-,
e" δ = 1.63 ppm , -C*H*$_2$-CH(C_6H_5)-,

Polybutadiene:
f, δ = 5.44 ppm -CH_2-C*H*=C*H*-CH_2- 1,4-*cis* and -*trans*;
f' δ = 5.6 ppm, 1,2 -CH_2-CH(C*H*=CH_2)- and δ = 4.99 ppm, -CH_2-CH(CH=C*H*$_2$)-;
f" δ = 2.1 ppm -C*H*$_2$-CH=CH-C*H*$_2$- and -CH_2-C*H*(CH=CH_2)-
f'" δ = 1.3-1.5 ppm, -C*H*$_2$-CH(CH=CH_2)-

Polyvinyl chloride:
g δ = 4.35-4.71 ppm, -CH_2-C*H*Cl-
g' δ = 2.11-2.52 ppm, -C*H*$_2$-CHCl-

Poly(vinyl acetate):
h δ = 4.92 ppm, -CH_2-C*H*($OCOCH_3$)-
h' δ = 1.98 ppm, -CH_2-CH($OCOCH_3$)-
h' δ = 1.83 ppm, -C*H*$_2$-C*H*($OCOCH_3$)-,

Poly(methyl acrylate):
i δ = 3.67 ppm, -CH_2-CH($COOCH_3$)-,
i' δ = 2.42 ppm, -CH_2-C*H*($COOCH_3$)-,
i' δ = 1.51-1.97 ppm, -C*H*$_2$-CH($COOCH_3$)-,

Polyacrylonitrile:
j δ = 4.35-4.71 ppm, -CH_2-CH(CN)-, **j'** δ = 2.2-2.28 ppm, -C*H*$_2$-CH(CN)-

References

1 Curran, D. P.; Bosch, E.; Kaplan, J.; Newcomb, M. *J. Org. Chem.* **1989**, *54*, 1826

2 Wrighton, M. S.; Ginley, D. S. *J. Am. Chem. Soc.* **1975**, *97*, 2065-2072.

3 (a) Balague, J.; Ameduri, B.; Boutevin, B.; Caporiccio, G. *J. Fluorine Chem.* **1995**, *70*, 215-223. (b) Balague, J.; Ameduri, B.; Boutevin, B.; Caporiccio, G. *J. Fluorine Chem.* **2000**, *102*, 253-268.

4 Wormald, P.; Ameduri, B.; Harris, R. K.; Hazendonk, P. *Polymer* **2008**, *49*, 3629–3638.

5 Guiot, J.; B. Ameduri, B.; B. Boutevin, B. *Macromolecules* **2002,** *35*, 8694-8707.

6 Pianca, M.; Barchiesi, E.; Esposto, G.; Radice, S. *J. Fluorine Chem*. **1999**, *95*, 71-84.

7 Fulmer, G. R.; Miller, A. J. M.; Sherden, N. H.; Gottlieb, H. E.; Nudelman, A.; Stoltz, B. M.; Bercaw, J. E.; Goldberg, K. I. *Organometallics* **2010**, *29*, 2176–2179.

8 Herman, X.; Uno, T.; Kubono, A.; Umemoto, S.; Kikutani, T.; Okui, N. *Polymer* **1997**, *38*, 1677-1683.

9 Bovey, F. A.; Jelinski, L. W.; Academic Press: New York, **1982**, p 157.

10 Ferguson, R. C.; Brame, E. G. *J. Phys. Chem*. **1979**, *83*, 1397-1401.

11 Russo, S.; Behari, K.; Chengji, S.; Pianca, M.; Barchiesi, E.; Moggi, G. *Polymer* 34, **1993**, *22*, 4777-4781

12 Timmerman, R.; Greyson, W.; *J. Appl. Polym. Sci.* **1962**, *6(22)*, 456-460.

13 David, G.; Boyer, C.; Tonnar, J.; Ameduri, B.; Lacroix-Desmazes, P.; Boutevin, B. *Chem. Rev*. **2006**, *106*, 3936–3962.

14 Boyer, C.; David, V.; Lacroix-Desmazes, P.; Ameduri, B.; Boutevin, B. *J. Polym. Sci.: Part A: Polym. Chem*. **2006**, *44*, 5763–5777.

15 Ameduri, B.; Ladavière, C.; Delolme, F.; Boutevin, B.; *Macromolecules* **2004**, *37*, 7602-7612.

16 El Soueni, A.; Tedder, J. M.; Walton, J. C. *J. Fluorine Chem.* **1978**, 11, 407—417

17 Duc, M.; Ameduri, B.; Ghislain, D.; Boutevin, B. *J. Fluorine Chem*. **2007**, *128*, 144–149.

18 (a) Koumura, K.; Satoh, K.; Kamigaito, M. *Macromolecules* **2008**, *41 (20)*, 7359-7367. (b) Koumura, K.; Satoh, K.; Kamigaito, M. *J. Polym. Sci.: Part A: Polym. Chem*. **2009**, *47*, 1343–1353.

19 Imran-ul-haq, M.; Beuermann, S. *Macromol. Symp*. **2009**, *275-276*, 102–111.

20 (a) Nagib, D. A.; MacMillan, D. W. C, *Nature*, **2011**, 224, 224-228. (b) Ji, Y.; Brueckl, T.; Baxter, R. D.; Fujiwara, Y.; Seiple, I. B.; Su, S.; Blackmond, D. G.; Baran, P. S. *Proc. Nat. Acad. Sci.* **2011**, *108*,14411–14415.

21 (a) Feiring, A. E.; Wonchoba, E. R.; Davidson, F; Percec, V; Barboiu, B. *J. Polym. Sci.: Part A: Polym. Chem.* **2000**, *38*, 3313–3335. (b) Kamigata, N.; Fukushima, T.; Terakawa, Y.; Yoshida, M.; Sawada, H. *J. Chem. Soc. Perkin Trans.* **1991**, 627-633.

22 Ameduri, B.; Billard, T.; Langlois, B. *J. Polym. Sci.: Part A: Polym. Chem*. **2002**, *40*, 4538–4549.

23 Shi, Z.; Holdcroft, S. *Macromolecules* **2004,** *37*, 2084-2089.

24 Modena, S.; Pianca, M.; Tato, M.; Moggi, G.; Russo, S. *J. Flourine. Chem*. **1989**, 43, 15-25

25 (a) Yang, Y.; Shi, Z.; Holdcroft, S. *Eur. Polym. J.* **2004**, *40*, 531–541. (b) Yang, Y.; Shi, Z.; Holdcroft, S. *Macromolecules*. **2004,** *37*, 1678-1681

26 Gilbert, B. C.; Kalz, W.; Lindsay, C. I.; McGrail, P. T.; Parsons, A. F.; Whittaker, D. T. E. *J. Chem. Soc., Perkin Trans. 1*, **2000**, 1187–1194.

27 Low, H. C.; Tedder, J. M.; Walton, J. C. *J. Chem. Soc., Faraday Trans. 1: Phys. Chem. Condens. Phases* **1976**, *72*, 1707.

28 Boyer, C.; Valade, D.; Sauguet, L.; Ameduri, B.; Boutevin, B. *Macromolecules* **2005**, *38*, 10353-10362.

29 Cape, J. N.; Greig, A. C.; Tedder, J. M.; Walton, J. C. *J. Chem. Soc., Faraday Trans. 1: Phys.Chem. Condens. Phases* **1975**, *71*, 592.

30 Drago, R. S.; Wong, N. M.; Ferris, D. C. *J. Am. Chem. Soc.* **1992**, *114*, 91-98

31 (a) Okafo, E. N.; Whittle, E. *Int. J. Chem. Kinet*. **1975**, *7(2)*, 287-300; (b) Ahonkhai, S. I. *Int. J. Chem. Kinet*. **1984**, *16(5)*, 543-58.

32 Anslyn, E. V.; Dougherty, D. A. *Modern Physical Organic Chemistry*, Chapter 16, *Photochemistry* p. 955-956, University Science Books, **2006**.

33 Pan, X.; Philbin, C. E.; Castellani, M. P.; Tyler, D. R. *Inorg. Chem.* **1988**, *27*, 671-676.

34 (a) Mamooda, Z.; Azama, M.; Mushtaqa, A.; Kausara, R.; Kausara, S.; Gilanib, S. R. *Spectrochim. Acta, Part A.* **2006**, *65(2*), 445-452. (b) Kaesz, H. D.; Bau, R.; Hendrickson, D.; Smith, J. M. *J. Am. Chem. Soc.* **1967**, *89*, 2844.

35 (a) Koumura, K.; Satoh, K.; Kamigaito, M. *Macromolecules*, **2008**, *41*, 7359. (b*)* Koumura, K.; Satoh, K.; Kamigaito, M. *J. Polym. Sci.: Part A: Polym. Chem*. **2009**, *47*, 1343. (c) Koumura, K.; Satoh, K.; Kamigaito, M. *Macromolecules* **2009**, *42*, 2497.